2023-08

Influence of duct configurations on the performance of solar-assisted heat pump dryer for drying tobacco leaves

Suleiman, Salum

NM-AIST

INFLUENCE OF DUCT CONFIGURATIONS ON THE PERFORMANCE OF SOLAR-ASSISTED HEAT PUMP DRYER FOR DRYING TOBACCO LEAVES

Salum Abdulkarim Suleiman

A Dissertation Submitted in Partial Fulfillment of the Requirements for the Degree of Master's in Sustainable Energy Science and Engineering of the Nelson Mandela African Institution of Science and Technology

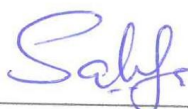**Arusha, Tanzania**

August, 2023

ABSTRACT

Inadequate storage facilities and preservation techniques lead to a decrease in the quality of agricultural products. Application of modern processing techniques has reduced post-harvest losses of agricultural crops. Drying was done to lower the moisture content for preservation. Tobacco drying requires massive amounts of wood, which has negative effects on the environment such as pollution, deforestation, and desertification. In the present study, a solar-assisted heat pump dryer (SAHPD) has been designed, fabricated and tested its performances as an alternative drying technology for tobacco leaves. The hot air generated from the solar collector and condenser unit of the heat pump was used as a source of heat in the drying chamber. In this study, we investigated thermal performance of three duct configurations of the SAHPD system (open, partially closed and completely closed) to establish the best configuration for drying tobacco leaves where did not conducted before. The average drying temperature was found to be 66, 64 and 60°C; the coefficient of performance of the heat pump was 3.4, 3.2 and 3.0; the heat energy contribution from the condenser was 98.7, 98.5 and 98.3%; and electrical energy consumption was 2.3, 2.8 and 2.6 kWh, for the open, partially and completely closed systems, respectively. Based on these results, the open system demonstrated the best performance. According to the study's findings, SAHPD has been shown to be an energy-efficient method of drying tobacco leaves and environmentally friendly as opposed to the conventional use of wood fuel, which results in environmental pollution, desertification, and deforestation. Future studies should focus on inclusive investigation of the life cycle and technoeconomic.

DECLARATION

I, **Salum Abdulkarim Suleiman**, do hereby declare to the Senate of the Nelson Mandela African Institution of Science and Technology that this dissertation is my original work and that it has neither been submitted nor being concurrently submitted for a degree award in any other institution.

Salum Abdulkarim Suleiman   25/08/2023

Name of Candidate   **Signature**   **Date**

The above declaration is confirmed by:

Dr. Thomas Kivevele   15/09/2023

Name of Supervisor 1   **Signature**   **Date**

Prof. Alexander Pogrebnoi   17.08.2023

Name of Supervisor 2   **Signature**   **Date**

COPYRIGHT

CERTIFICATION

The undersigned certify that, they have read and hereby recommend for acceptance by the Nelson Mandela African Institution of Science and Technology a dissertation titled *"Influence of duct configurations on the performance of solar-assisted heat pump dryer for drying tobacco leaves"* in partial fulfilment of the requirements for the degree of Master's in Sustainable Energy Science and Engineering of the Nelson Mandela African Institution of Science and Technology.

Dr. Thomas Kivevele

Name of Supervisor 1   **Signature**   **Date**

15/09/2023

Prof. Alexander Pogrebnoi

17.08.2023

Name of Supervisor 2   **Signature**   **Date**

ACKNOWLEDGEMENTS

DEDICATION

My dedication goes to my family specifically my wives, my mother and father, my sons and daughter, brothers and sister for their constant support and for not taking my absence for granted.

TABLE OF CONTENTS

LIST OF TABLES

LIST OF FIGURES

LIST OF APPENDICES

LIST OF ABBREVIATIONS

A_c — Area of solar collector

COP — Coefficient of performance

COP_{hp} — Coefficient of performance of heat pump

$COP_{Overall}$ — Overall coefficient of performance

C_{pair} — Specific heat capacity of air

E_{com} — Compressor electrical energy

FC — Fully closed

FO — Fully open

HP — Horse power

Hp — High pressure

HPD — Heat pump dryer

I — Line current

I_T — Solar radiation incident on the collector

LP — Low pressure

$\dot{m}_{air}$ — Air mass flow rate

MC — Moisture content

M_{water} — Mass of water evaporated

P — Pressure instrument

PC — Partial closed

P_{fans} — Power consumed by the fan

Q_u — Useful energy gain by the collector

SAHPD — Solar collector assisted heat pump dryer

SMER — Specific moisture extraction rate

TORITA — Tobacco Research Institute of Tanzania

$T_{o,coll}$ — Outlet air temperatures of solar collector

$T_{i,coll}$ — Inlet air temperatures of solar collector

$T_{o,cond}$ Outlet air temperatures of condenser

$T_{i,cond}$ Inlet air temperatures of condenser

t_1, t_2 Time consumed by solar at a certain period

V   Line Voltage

η_c Solar thermal efficiency

CHAPTER ONE

INTRODUCTION

1.1   Background of the Problem

For many years, drying of biomaterial products has been used for preservation, most of the harvested products have high moisture content which is difficult for storage and maintenance for later uses (Alishah *et al.,* 2018; Vickers, 2017). Therefore**,** drying is a crucial process in many food industries and agricultural-based economy countries to maintain quality without deteriorating biomaterial products, sum up the original taste, and uphold the nutrition values (Chua & Chou, 2014a). The main objective of drying is not only to remove moisture from the product where bacteria and yeast can grow and spoil the product but also to preserve the initial properties of the products (Sagar & Kumar, 2010; Liu *et al.,* 2013a). The operating process of the dryer is to transfer heat from the source to the product and then to the environment. The structure of biomaterials in the drying process is changed by heating and causing moisture in the work to vaporize and change the layout. In various investigations it has been demonstrated that the drying process has high energy consumption, in agriculture is 60%, while in wood is around 70% (Şevik, 2014a). For example, an average of 14 kg of wood fuel is consumed to obtain 1 kg of cured tobacco leading to a deforestation rate of 13 000 hectares per annum in Tanzania (Msigwa, 2019). In efforts to combat this threat, the Tobacco Research Institute of Tanzania (TORITA) has managed to come up with rocket barns that use less wood, 7 cubic meters, to cure leaf tobacco compared to local barns that use 19 cubic meters of wood. This is a remarkable achievement in the tobacco sector as the calorific value of wood is still higher for curing tobacco compared to other identified organic briquettes that have already been tried. However, the tested barns are still inefficient, use wood fuel, and cause emissions. The TORITA is therefore exploring an alternative curing source apart from wood, primarily renewable.

Besides, more efforts are taken on using renewable energy and other high-efficiency drying technologies. Many researchers suggest the use of heat pump dryers because of their high efficiency and energy-saving potential and less negative impact on the environment due to greenhouse gases produced by fossil fuels and wood burning which leads to global warming (Chua & Chou, 2014b). However, solar dryers fail to operate when there is no active sunlight in case heat storage systems are not integrated into them. Sometimes even if heat storage

1

systems are integrated, there are challenges related to the selection, cost, availability, and efficiency of storage materials. Heat pump dryers have been used in many countries to dry biomaterials that are sensitive to heat, and the process is controllable (Liu *et al.,* 2013b; Şevik, 2014b; Lingayat *et al.,* 2020). The quality, color, and smell of the product dried by the heat pump are better than the product dried with other drying technologies such as open sun drying (Jimu *et al.,* 2017). In order to increase the performance of the heat pump dryer and lower operating costs, solar collectors are integrated into the heat pump system to form a solar-assisted heat pump dryer (SAHPD) (Liu *et al.,* 2013b; Şevik, 2014b).

The SAHPD application provides high energy efficiency with controllable temperature, airflow, air humidity, and enormous energy-saving potential. The application of heat pump drying technology in tobacco manufacturing has been reported elsewhere with an energy-saving potential from 20% to 50% (Newbert, 1985; Ratner *et al.,* 2020). The SAHPD can exhibit a coefficient of performance (COP_{hp}) as high as four meaning that 1 kW of electric energy is needed to have a release of 4 kW of heat at the condenser for drying applications. A high COP value represents high efficiency and also equates to lower operating costs. This technology is uncommon in most African/developing countries; however, developed countries have been using it at an advanced stage based on their specific climatic conditions which cannot directly be applied to different regions. The SAHPDs are affected by the change in ambient conditions, proper configuration of the duct is therefore a key in improving the performance of the dryer (Şevik, 2014b; Yahya *et al.,* 2023). To the best of the authors' knowledge, the influence of duct configuration on the performance of the SAHPD is not well documented. The objective of the present study is therefore to investigate the influence of duct configurations (open, partially closed, and completely closed air ducts) on the thermal performance of the SAHPD to establish the best configuration for drying tobacco leaves in tropical climate on the base of drying temperature, COP_{hp}, and electrical energy consumption.

1.2 Statement of the Problem

The tobacco sector in Tanzania is being accused of destroying forests by cutting trees to obtain wood for curing tobacco leaves, causing a threat of deforestation and global warming in the country. Therefore, this study is proposing a Solar Collector-Assisted Heat Pump Dryer (SAHPD) technology for drying tobacco leaves and other biomaterials such as fruits and vegetables as alternative way to minimize the deforestation and global warming. This technology is uncommon in Tanzania; however, it has been used in developed countries but

was not applied regarding Tanzanian specific climatic conditions. Most of the researcher's reported the performance of heat pump dryers with a focus on optimization of the drying parameters (drying air temperature, airflow rate, and relative humidity). However, the overall performance of the heat pumps drying system, which consists of two subsystems-the heat pump and the drying system-depends upon working conditions, and the two subsystems interact with each other while connected with air duct. Different duct configurations can influence the performance of the dryer. Thus, the heat pump and the dryer should not be examined or optimized separately because any change of working parameters at one system, significantly affects the performance of the other system. In this study, therefore, SAHPD will be developed and evaluated for its performance as a single integrated system for drying tobacco leaves with the focus on the influence of duct configurations.

1.3   Rationale of the Study

The study is conducted on climatic condition of Arusha, the study of the background of tobacco drying were taken on some area that plant the tobacco but not all of them because of Covid-19. The Covid-19 was the big problem which overcome to stop visiting most area of the study and cause to finish out of the time. Therefore, more research needed in different area and climatic condition for investigate the performance of the drying of the tobacco.

1.4   Objectives of the Study

1.4.1   General Objective

To investigate the influence of duct configurations on the performance of solar-assisted heat pump dryer for drying tobacco leaves.

1.4.2   Specific Objectives

The study aimed to achieve the following specific objectives:

(i)   To develop solar-assisted heat pump dryer for drying tobacco leaves.

(ii)   To carry out thermodynamic analysis of the developed solar-assisted heat pump dryer and identify factors responsible for the inefficiency of the system.

(iii)   To evaluate the influence of three air duct configurations (open, partially, and fully closed) on the performance of solar-assisted heat pump dryer.

1.5   Research Questions

The study intended to answer the following questions:

(i)   To what extent the developed solar-assisted heat pump dryer from drying tobacco leaves can perform well.

(ii)   How could improve the performance factor for inefficiency of the dryer system?

(iii)   Which configuration of solar-assisted heat pump dryer has maximum out performance?

1.6   Significance of the Study

Whatever the standard and improved barns benefits, still there are ample research and improvement opportunities, especially in those aspects related to reducing energy consumption like the use of solar energy, which is abundant in Tanzania.

Tobacco leaves drying system will attract government and other stakeholders to invest in developing sustainable, simple to operate, reasonable cost, high-efficiency products and suitable for small-scale farmers.

Since the SAHPD does not use a wood material and receives direct sun rays and is assisted by electricity for heat pump operation. Therefore, the use of these drying systems is essential for developing sustainable sources of reducing energy consumption and environmental impact.

1.7   Delineation of the Study

The study covers only the drying of tobacco leaf products in Tanzania; the curing of tobacco processes of coloring, color fixing, leaves, and midrib drying; and removing the moisture from the system. A solar-assisted heat pump dryer is a dryer that operates due to heat generated by a solar collector and heat pump as an assistant to the system. The study evaluated the overall performance of solar-assisted heat pump dryer configurations i.e., open, partially closed, and completely closed air duct systems. Different parameters such as temperature, moisture, and weight of the product are considered for performance during the system operation.

<div style="text-align:center">

CHAPTER TWO

LITERATURE REVIEW

</div>

2.1 Types of Curing Barns

For many years**,** tobacco leaf was dried for further uses and different types of burns, such as solar assisted barns, rocket barns or alternative dryer**s** were applied in various countries.

2.1.1 Solar Assisted Barns

Solar assisted tobacco curing barns are one of the most prominent alternatively powered curing barns. Solar barns use radiation from the sun as passive heating for an auxiliary heating source to power the barn. There are two different tactics used to harness the radiation: i) solar energy collecting installations and ii) multifunction barns that use a greenhouse effect (Fara *et al.,* 1985). The heat is then actively transported to a central location and either directly used for heating, preheating outdoor air, or stored, often in a rock bed (Fara *et al.,* 1985).

2.1.2 The Rocket Barn

The rocket barn is an energy efficient curing barn that was invented in Malawi in 2006 by biomass energy consultant Peter Scott in collaboration with Hestian Rural Innovation Development (HRID), Total Land Care, and the Program for Biomass Energy Conservation (ProBEC) (Munanga *et al.,* 2014). The design goals were to develop an easy-to-construct, affordable curing barn that would a) increase efficiency, b) increase the quality of tobacco products, and c) reduce the time required to cure tobacco, thus increasing the barn capacity (Munanga *et al.,* 2014). The third generation Rocket Barn has demonstrated a 54.3% energy saving in small-scale barns. In 2009, a Malawian farmer growing 1 hectare of tobacco spent an average of $285 USD, or 23% of the cost of production, on firewood for curing (Kägi and Schmid, 2010). The Rocket Barn has also demonstrated a 19% decrease in curing time and 44.1% increase in the value of the product (Munanga *et al.,* 2014). A commercial-sized Rocket Barn yields even greater energy savings of up to 75%, with a minimum of around 1.5 (Kägi and Schmid, 2010; deSolaPool, 2009). Therefore, curbing deforestation from the curing tobacco process is a forestation due to tobacco regulations or growing trees to be harvested for firewood, and every farmer should have afforested trees for the curing process. British American Tobacco and other tobacco companies, such as Imperial Tobacco, have launched

<div style="text-align:center">

5

</div>

forestation campaigns around the world (Chacha, 2000). The wood is too expensive to transport, and often the farmers have no feasible access, but has even acknowledged that afforestation programs are not necessarily in the same general locations as the farmers are continuing with their behavior of cutting the natural forests. Therefore, if users of the Rocket Barn are not sourcing their wood sustainably, they will decrease their wood consumption but still contribute to global deforestation in the curing process.

2.1.3 Alternative Dryer

There are various approaches to curb deforestation from curing tobacco. A contrasting approach to utilizing alternative fuels is to increase the energy efficiency of the dryer. Solar collector assisted heat pump dryer is major way to eliminate the deforestation, minimize greenhouse gas, increasing quality and performance of dryer. This alternative will not use a fossil fuel and wood, only solar collectors assisted and heat pump as a source of heat (Kaewkiew *et al.,* 2012). Heat pump systems are more economical and recovering heat from different sources, and used in commercial and residential applications (Chou & Chua, 2001). Heat pump drying has ability to use the latent and transfer to drying air which can operate even under humid ambient condition with low cost and minimum environmental pollution (Mujumdar, 2006).

In addition, a summary of past research works on heat pump dryers and SAHPD are provided in Tables 1 and 2 in terms of study location, type of the studied biomaterials and conclusions of their findings. In general, heat pump drying is a technology by which materials can be dried at low temperatures and in an oxygen-free atmosphere, using less energy. Heat pump drying is therefore advantageous for drying biological materials which are thermally sensitive and oxygen sensitive, such as tobacco leaves, fruits and vegetables. As discovered in the literature, the advantages of heat pump dryers are exceptional and can be recommended as an efficient method for drying industries. It has been reported that 6% of primary energy could be saved if heat pumps are used to their full technical potential for water heating and other industrial applications such as drying. Heat pump drying is a more advanced method than the well-known drying methods such as direct/indirect sunlight. Although this method (direct/indirect sunlight drying) is cheap, there are problems associated with it, such as poor quality of dried products; no control over the drying process; possible contamination of the product by dirt, rodents, animals, infestation by insects or moulds as well as exposure of the product to rain and wind resulting in repeated wetting and re-drying (Kivevele & Huan, 2014a). Thus, in case of efficient

use of direct sunlight for drying purposes it is imperative to integrate solar collector with heat pump system. Heat pump dryers integrated with solar collectors provide high energy efficiency with controllable temperature, air flow and air humidity and have significant energy-saving potential. The SAHPD is technology comes to minimize the energy consumption and increasing performance of the drying performance and maintain the quality of the dried product as shown on Fig. 1 (Singh *et al.,* 2020c).
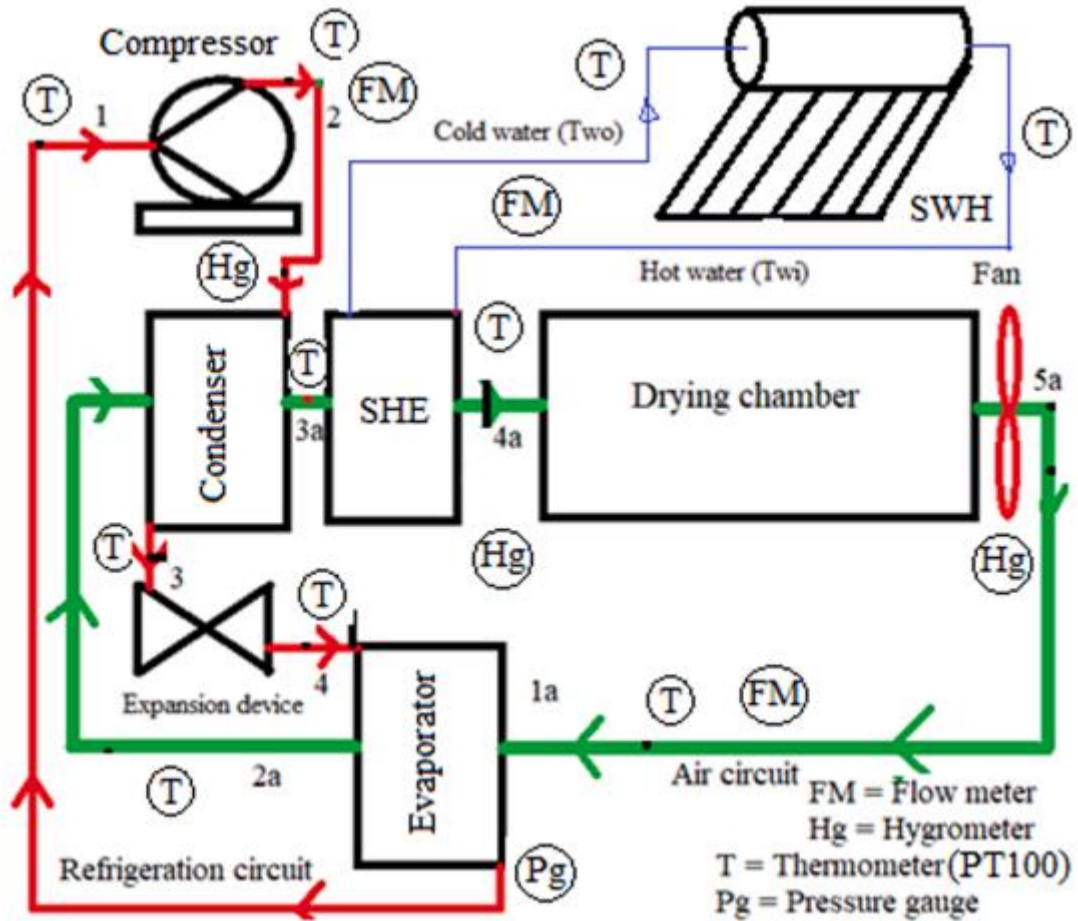
Figure 1: **Schematic diagram of the previous study on SAHPD system (Singh *et al.,* 2020a)**

Table 1: **Summary of studies on heat pump dryers (Kivevele & Huan, 2014b)**

Location	Application (s)	Comments	Reference
Singapore	Green beans	Coefficient of performance (COP) value of above 6 was observed and a Specific Moisture Extraction Rate (SMER) value above 0.65 for a material load of 20 kg and compressor speed of 1200 rpm was obtained.	Hawlader and Jahangeer (2006) and Hawlader *et al.* (2003)
Singapore	Agricultural and marine products	With scheduled drying conditions the quality of products can be improved.	Chou *et al.* (1998) and Chua *et al.* (2000)
Australia	Grain	An open cycle Heat Pump Dryer (HPD) performed better during the initial stage when the product drying rate is high.	Theerakulpisut (1990)
South Africa	Grains	The HPD is more economical than other dryers.	Meyer and Greyvenstei (1992)
Brazil	Vegetable (Onion)	Better product quality and energy saving of the order of 30% was obtained.	Jangam and Thorat (2010)
Australia	Macadamia nuts	The high quality of dried nuts was observed	Str∅mmen and Kramer, (1994)
New Zealand	Apple	Modified atmosphere HPD (MAHPD) produced products with a high level of open pore structure, contributing to the unique physical properties.	O'Neill *et al.* (1998)
Thailand	Garlic and White mulberry	Computer simulation model of the heat pump dehumidified drying shown to be in good agreement with experimental results.	Phoungchandang (2009)
Iran	Plum	The optimum temperature of drying for plums is in vicinity of 70 - 80ºC; also, the SMER of	Chegini *et al.* (2007)
Indonesia	Red Chillies	The high quality of the dried chillies was highlighted as the major advantage of HPD compared to sun drying.	Tjukup *et al.* (2012)

Table 2:   Summary of studies on solar assisted heat pump dryers

Location	Application (s)	Comments	Reference
India	Banana and potato chips.	The study considered the comparison between SAHPD and HPD, and the study reveals that the SAHPD system is much better than the simple HPD system	Singh *et al.* (2020a)
India	batch-type solar-infrared assisted heat pump dryer is developed and experimentally investigated for closed air cycle drying of banana chips.	The COP of simple HPD was better as compared to others. Average COP of simple HPD, IAHPD, SAHPD, and SIAHPD were 2.618, 2.303, 2.04 and 1.94, respectively.	Singh *et al.* (2020b)
India	Banana chips	The COPWS of SAHPD was better than HPD system. The average values of COPWS of HPD and SAHPD were 2.04 and 3.43, respectively.	Singh *et al.* (2020c)
Thailand	Drying chili peppers	The study was comparison between SAHPD and traditional drying method.It was found that the SAHPD with recovery gave better drying performance than a traditional dying method.	Naemsai *et al.* (2019)
China	shiitake mushroom,	(Xu *et al.,* 2021)	
Indonesia	paddy and its product quality	The study to assessed the drying performance of a hybrid solar-assisted heat pump dryer (HS-AHPD). Due to the higher head rice yield (93.10 1.044%), lower broken rice (4.41 0.737%), and lower rice grouts (1.11 0.271%) after drying, the products were of better quality.	Yahya *et al.* (2023)
Columbia	state of the art, drying kinetics, and product qualities	A review of the state-of-the-art, drying kinetics, and product characteristics for solar and sun-assisted drying of fresh food, In comparison to other sun dryers, hybrid solar drying results in higher drying rates and product quality.	Boateng and Agriculture, (2023)

CHAPTER THREE

MATERIALS AND METHODS

3.1   Materials and Equipment

The SAHPD is the system where the solar collector and heat pump which consists of four main components: condenser (Cond), evaporator (Evap), compressor (Comp), and expansion valve (Exp. valve) were integrated together as a source of heat in a drying process of biomaterial products. Other components like air blowing fans, drying chamber, and duct as air flowing path were used to support the workflow of the SAHPD as shown in Figures 2 and 8.
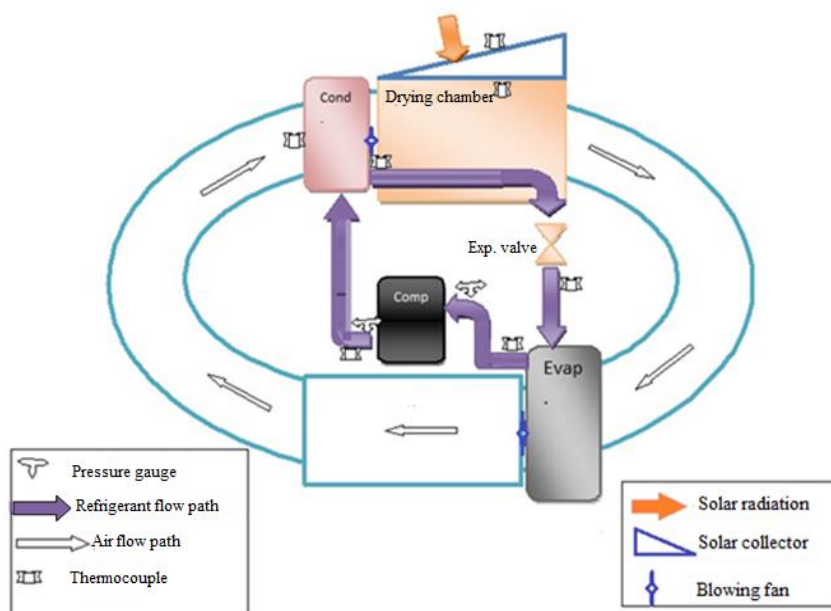
Figure 2:   Schematic diagram of fully closed SAHPD

3.1.1   Solar Collector

The solar collector was designed as a passive gain system which was made of an absorbing black painted plate, transparent glass plate of $946 \times 946 \times 6$ mm size, and was integrated with the drying chamber as depicted in Figure 5. The frame of the solar collector was made of a mild steel sheet of 1.5 mm thickness and insulated by fiberglass materials; inside the surface of the chamber is painted black. The solar collector was inclined at 13 degrees facing north and placed on the top of the drying chamber to heat the biomaterial in the drying chamber. At the top of the glass, a cover of movable plywood was placed and used to isolate the solar irradiance entering the drying chamber when necessary.

3.1.2 Heat Pump

The heat pump is composed of a Danfoss reciprocating compressor, 4 horsepower condensers, and evaporator with two built-in fans of 186 W, 0.88 A (Figure 3), and an expansion valve (3/8 × 1/2 inch) from Denmark which is used as the pressure reducing device; the refrigerant expands and its temperature reduces. All components are connected with 3/8- and 5/8-inch copper tubes to form a single unit. The heat pump operates under refrigerant R134a (1,1,1,2-tetrafluoromethane). The refrigerant is pumped directly from the liquid receiver by the compressor in the high-pressure side, the pressurized gas passes through the condenser/heat exchanger where air entering the dryer is heated-up through heat exchange between cold air passing through the surfaces of the hot copper pipes carrying hot refrigerant. The air is circulated in the system using built-in fans at the condenser and evaporator. When the latent heat of condensation of the refrigerant at the condenser is evolved, the pressured gas is condensed and accumulated at the vertical liquid receiver. The refrigerant then passes through the expansion valve which is used as the system's refrigerant control to the evaporator, creating a pressure drop and accumulating in the refrigerant receiver and then back to the low-pressure side of the compressor to complete the circulation.

For the construction of the SAHPD, the following materials available in the local market were used: tempered steel sheet and clear glass, angle irons of 25×25×3 and 50×50×6 mm dimensions, and the aluminum rod of 40 mm diameter. The compressor and its accessories like the liquid receiver, oil receiver, and refrigerant receiver is shown in Figure 3a. The heat pump system consists of a condensing unit, evaporator, expansion valve, and a compressor unit integrated with oil and liquid/refrigerant receivers as depicted in Figure 3, and more details are summarized in Table 3.

(a) (b) (c)
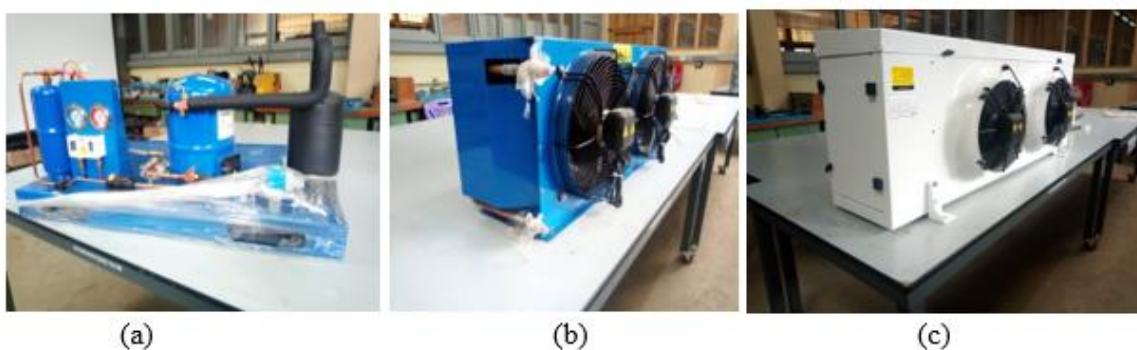
Figure 3:   Compressor unit (a), Condenser unit (b), and Evaporator unit (c)

3.1.3 Duct

The duct system was made of a mild steel sheet of 1.5 mm thickness and reinforced by angle iron of 25×25×3 mm as seen in the section diagram (Fig. 4). The specification and functions of the equipment accessories are summarized in Table 3.
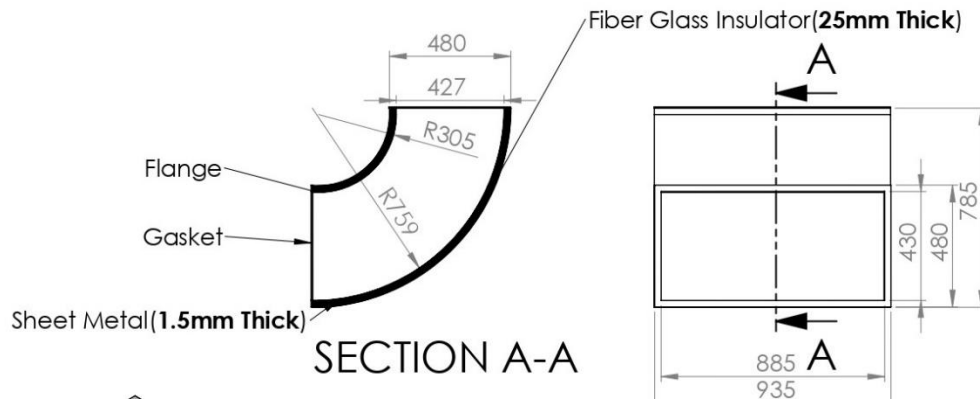
Figure 4: **Section diagram of the elliptic duct**

3.1.4 Drying Chamber

The drying chamber was a batch type unit made of mild steel of 1.5 mm thickness and reinforced by angle iron of 25×25×3 mm for connection which was mounted with M8 and M10 bolts. The chamber was mounted on a frame made of angle iron of 50×50×6 mm; at the top, it was mounted with clear glass, and one side was connected directly to the insulated duct and the other side to the condenser as seen in section diagram (Fig. 7). The duct is connected to the evaporator, condenser, and drying chamber as depicted in Figs. 1 and 2. Inside the chamber, the aluminum rod of a 40 mm radius was used as a supporter for racks on which tobacco leaves were placed (Figs. 5 and 6).

Figure 5: **Drying tobacco leaf inside the drying chamber**

Figure 7 shows the complete drying chamber integrated with a direct gain solar collector/ solar glass on the top. A plywood sheet was used to slide up and down through the glass cover rail for isolating the solar collector when only the heat pump dryer was tested. Weight scale was placed at the bottom of the drying chamber and attached to the hanger using aluminium rod for continuously measuring the weight loss of the drying products.

Figure 6:   Section diagram of drying chamber with a solar collector

3.1.5   Equipment Specifications and Functions

The equipment and accessories used for measuring temperature, pressure, relative humidity, solar radiation, and other accessories used in the SAHPD are summarized in Table 3.

Table 3:   Equipment accessories

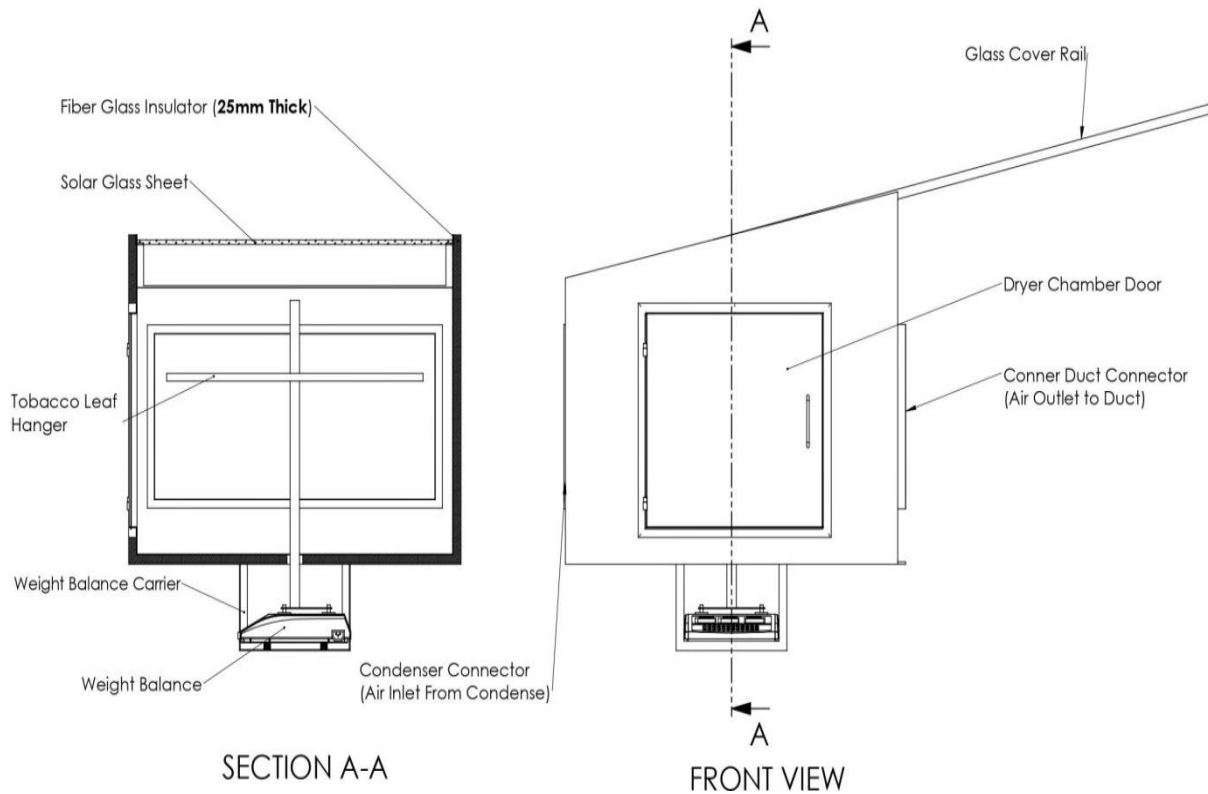| S/N	Equipment	Specification	Function
1.	Thermocouples	Model: T-type Max measuring temperature: 120 °C and above.	To measure the ambient and drying temperature, inlet and outlet evaporator, collector, and condenser temperature.
2.	AC Digital Display Power Monitor Meter.	Voltage: 80~260 VAC Rated current and power: 100 A, 22 kW, operating frequencies 45–65 Hz.	To measure the voltage, rated power, and frequency.
3.	FST200 Digital RS4850 10 V 0–5 V, Wind Speed Sensor Anemometer Data Logger.	Model FST200-201+211 operating wind speed range 0.5~50 m/s.	To measure the air speed inside the drying chamber.
4.	21CFR Part11 Compliant USB Temperature and Humidity Data Logger Recorder with Free Software.	Model EL-21CFR-2-LCD, operating temperature range from –35 to +80 °C and relative humidity range 0 – 100%.	Measuring temperature and relative humidity inside the drying chamber.
5.	Pressure gauge.	Model CLASSES I.6 made by the XMK Company.	Used to measure the pressure in the high-pressure side and low-pressure side.
6.	Weight balance.	MX1925.	Measuring the weight of tobacco leaves in the drying chamber.
7.	Danfoss reciprocating compressor	4 HP (MTZ36GJ5EVE, LR70 A thermal protect, Low pressure side is 22.6 bar, high pressure side 29.4 bar).	Used for circulating refrigerant in the heat pump system
8.	Expansion valve	R134a Danfoss (TEN2 R134a, 068Z3348, -40/+10 °C/-40/+50 °F).	Used as refrigerant control in a system.
9.	Condenser	4HP with 102 mm×450 mm×300 mm dimension with two adjustable fans of 175 W, 0.75 A, and 1335 rpm.	Used to condense the refrigerant vapor to liquid and for heating air entering the drying chamber
10.	Evaporator	4HP with the size of 1020 mm×510 mm×400 mm	Used as a heat absorption part in the system when the refrigerant passed through at low temperature and pressure.
11.	Refrigerant R134a	13.6 kg.	Used as the refrigerant in the heat pump system.
12.	Solar Power Meter	SM206	Used to measure solar irradiance.
13.	Fans	175 W, 0.75 A and 1335 rpm, and 186 W, 0.88 A.	Used to circulate air in the system.

3.2 Experimental Procedure

3.2.1 Three Configurations of SAHPD

The SAHPD was designed in three duct configurations; fully closed, partially closed, and fully open as seen in Figs. 1, 6a, and 6b, respectively. In the fully closed configuration, the air duct connects the evaporator directly with the condenser; there is no interaction between drying air and the environment, and the drying air circulates within the system without interruption as seen in the section diagram of a complete SAHPD system (Fig. 8). In the partially closed configuration, there are gaps in the duct; the external air and drying air are mixed and used as inlet drying air as shown in Fig. 7a. The fully open system draws air from the fan through the evaporator and discharges air to the other end of the evaporator. It also draws the surrounding air through the condenser where it is heated and passes through the drying chamber; the moist air is discharged into the environment as shown in Fig. 6b. In this study, several parameters like output and input temperatures of the collector ($T_{o,coll}$, $T_{in,coll}$) and condenser ($T_{o,cond}$, $T_{in,cond}$), ambient temperature ($T_{ambient}$), pressures, humidity, electrical energy, solar energy, air speed, the weight of tobacco, were measured during the experiments and these parameters were used to determine the coefficient of performance, energy consumption, and moisture content. The solar meter was used to measure solar irradiance with the solar sensor placed on a tilted position on the top of the solar collector surface and the readings were recorded every 30 min; the thermocouple, and multimeter were used for electrical measurements. Utilizing a weighing scale, the refrigerant R134a of 5.9 kg mass was loaded into the heat pump system; a pressure gauge was used to measure and fix pressure at the high- and low-pressure sides, 49 and 19 bar, respectively. Tobacco leaves of the same weight (15 kg) were dried in the SAHPD for each configuration. In order to maximize the thermal performance of the SAHPD, the condenser fan was run at 950 rpm from a maximum speed of 1330 rpm, and the evaporator fan was run at a minimum speed below the rated speed of 1335 rpm to reduce the cold air flowing speed that was because it was affecting the drying process in partially and fully closed systems. In every 30 min, the weight of the tobacco was recorded. In each experiment, sixteen measurements were taken per day. Overall, it took five weeks to complete the measurements for the aforementioned configurations, including testing, installing, and removing some components.
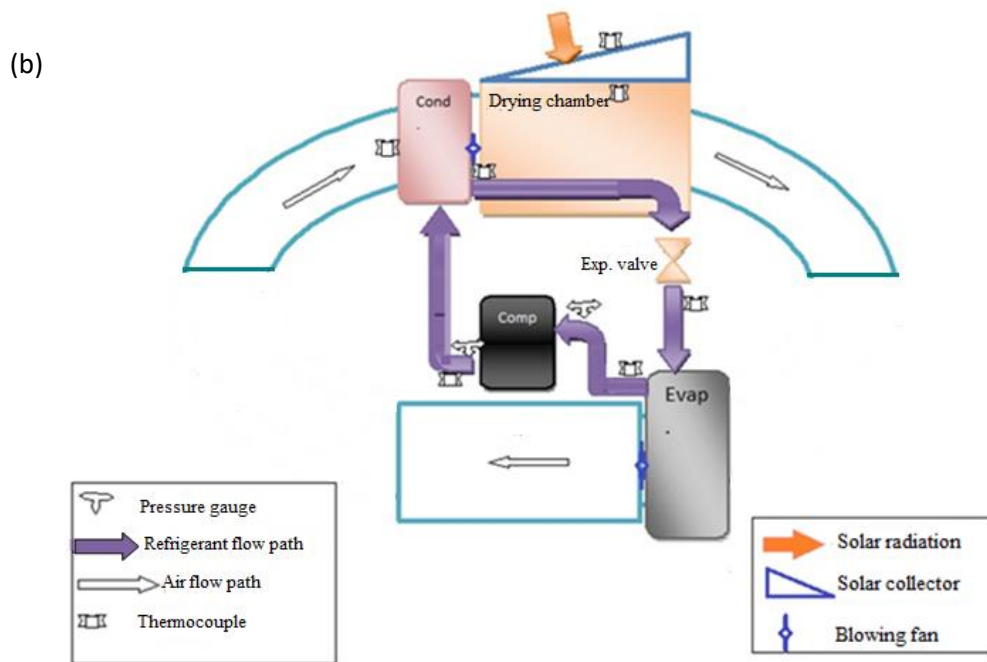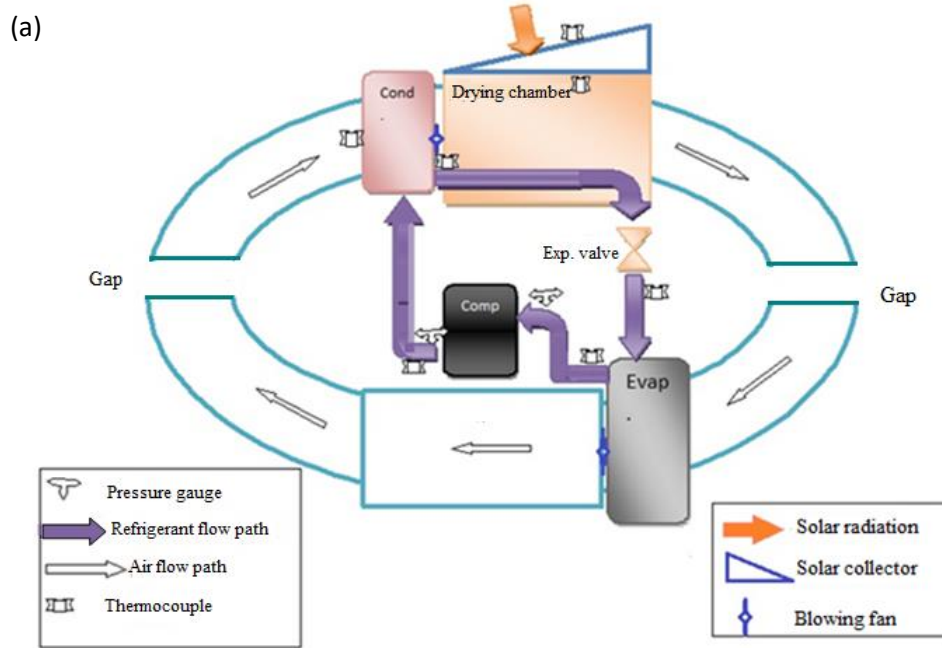
(a)

(b)

Figure 7: **(a) Partially closed SAHPD, and (b) partially closed SAHPD**
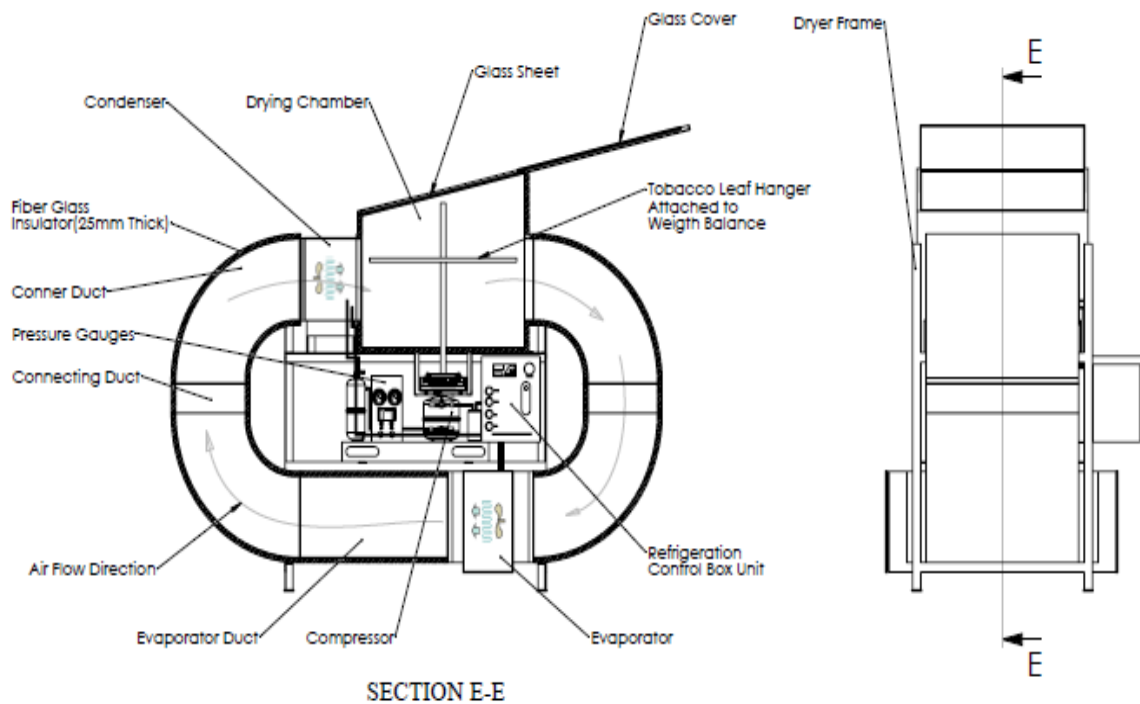
SECTION E-E

Figure 8: **Section diagram of a complete solar-assisted heat pump drying system**

The drying process in the developed SAHPD employed all modes of heat transfer such as radiation, convection, and conduction. The solar collector received direct heat of short wave radiation from the sun; the collector generates the long wave radiation which combines with heated air generated from the condenser in the drying chamber (Naemsai *et al.,* 2019).

Convective hot air drying involves blowing hot air over the moist products in the drying chamber. Conduction, convection, and phase change are responsible for the heat transmission from the product's surface to its inside. Mass transfer takes place through evaporation from the surface of the products to the environment as a result of the constant supply of heat energy. In addition, due to concentration gradients, internal mass transfer happens via diffusion capillary flow and viscous flow within the products (Naemsai *et al.,* 2019).

3.2.2   Evaluation of the SAHPD Performance

The SAHPD performance was evaluated through analysis of the following parameters: energy consumption, solar thermal efficiency, vapor compression in the heat pump, and efficiency of the drying chamber. All temperatures that were recorded were used in different calculations.

3.2.3 Solar Thermal Efficiency

The solar thermal efficiency (η_{coll}), defined as the ratio of usable heat collected by the solar collector to the solar radiation received on the collector surface for a certain period, was calculated as follows (Kaewkiew *et al.*, 2012):

$$\eta_{coll} = \frac{\dot{m}_{air} C_{pair}(T_{o,coll} - T_{in,coll})}{I_T A_c} \times 100 \tag{1}$$

where $\dot{m}_{air}$ is air mass flow rate, C_{pair} is the specific heat capacity of air, $T_{o,coll}$ and $T_{i,coll}$ are outlet and inlet air temperatures of solar collector, I_T is solar radiation incident on the collector, A_c is the area of solar collector.

3.2.4 Performance of the Vapor Compression Heat Pump

The performance of the vapor compression heat pump cycle was determined in terms of coefficient of performance (COP_{hp}). The COP_{hp} is the ratio of the heat rejected from the condenser to the compressor work input. The COP_{hp} of the heat pump cycle was calculated through the following equation (Technoheaven):

$$COP_{hp} = \frac{Q_{ucond}}{W_{comp}}, \tag{2}$$

that is

$$COP_{hp} = \frac{\dot{m}_{air} C_{pair}(T_{o,cond} - T_{i,cond})}{E_{comp}} \tag{3}$$

where air mass flow rate

$$\dot{m}_{air} = A_{dc} \rho_a V_{air}. \tag{4}$$

$T_{o,cond}$ and $T_{i,cond}$ are the outlet and inlet air temperatures of the condenser, E_{comp} is the electrical energy consumed by the compressor. The A_{dc}, ρ_a, and V_{air} are the area of drying chamber, air density and air velocity, respectively. The integration of a heat pump system together with the solar collector into the dryer requires additional energy-consuming units, namely, the fans and evaporator. All the energy input to this system should be included in the calculations. Therefore, the coefficient of performance of the overall system ($COP_{overall}$) of the SAHPD was determined according to following equation (Singh *et al.*, 2020a):

$$COP_{overoll} = \frac{Q_{ucond}+Q_{ucoll}}{E_{comp}+E_{fan}} \qquad (5)$$

where Q_{ucond} is the energy consumed by the condenser and Q_{ucoll} is useful energy gained by the collector, and E_{fan} is the energy consumed by the fan.

Specific moisture extraction rate SMER which shows dehydration quantity $\dot{m}_{water}$ per unit of energy consumed was calculated by the following equation (Hawlader *et al.,* 2006; Huy, 2018):

$$SMER = \frac{\dot{m}_{\dot{m}water}}{E_s+E_{comp}+E_{fan}} \qquad (6)$$

where E_s is the energy incident onto the plane of the solar collector.

3.2.5 Performance of Drying Chamber

The moisture content *MC* of the tobacco leaves was calculated using the following equation (Hawlader *et al.,* 2006):

$$MC = \frac{m_i-m_t}{m_i} \times 100 \qquad (7)$$

where m_i and m_t is the initial weight of the sample, m_t is the weight of the sample at a recorded time, respectively. The drying rate *DR* is the mass of water *m* evaporated from the wet tobacco leave per unit time. It was defined using the following equation (Shanmugam & Natarajan, 2007):

$$DR = \frac{m_{t+dt}-m_t}{dt} \qquad (8)$$

The mass of the water evaporated from wet tobacco leaves can be calculated according to Srisittipokakun *et al.* (2012) as:

$$m = \frac{M_{wetT}(MC_i-MC_f)}{(100-MC_f)} \qquad (9)$$

where M_{wetT} is the initial mass of wet tobacco leaves, MC_i is the initial and MC_f is the final moisture content.

The thermal efficiency of a dryer is the ratio of the energy used for moisture evaporation to the energy input to the drying system. It was calculated according to Shanmugam and Natarajan, (2007) as follows:

19

$$\eta_{dryer} = \frac{\dot{m}_{\dot{m}_{water}} H_{lv}}{E_s + E_{comp} + E_{fans}} \tag{10}$$

where H_{lv} is the latent heat of the vaporization of water.

The energy efficiency is the ratio of the energy consumed of the product from the drying product to the total energy input in the system and given by Singh *et al.* (2020a):

$$\eta_{energy} = \frac{m_w H_{lv}}{t_d (W_{comp+} + W_{fan})} \tag{11}$$

where m_w is the mass of water removed from the product, and t_d is the drying time.

The percentage of heat energy contribution by the solar collector *HEC*$_{coll}$ and condenser *HEC*$_{cond}$ was calculated using the following equations (Kush, 1980):

$$HEC_{coll} = \frac{Qu_{coll}}{Qu_{coll} + Qu_{cond}} \times 100, \tag{12}$$

$$HEC_{cond} = \frac{Qu_{cond}}{Qu_{coll} + Qu_{cond}} \times 100 \tag{13}$$

where Q_{ucoll} is the useful heat gained by the solar collector and Q_{ucond} is the useful heat or heat energy released by the refrigerant in the condenser.

3.3   Uncertainty of Investigation Result

Uncertainty analysis is the essential analysis in any experimental work to support the obtained results, according to Singh *et al.* (2020a). Let Y represent the result and ($z_1, z_2, z_3, ..., z_n$) are independent variables of the function. Thus,

$$Y = Y(z_1^{u1}, z_2^{u2}, z_3^{u3}, ..., z_n^{un}) \tag{14}$$

Let Q_R is the uncertainty and Q_1, Q_2, Q_3, ..., Q_n are the uncertainty variables; then the estimated uncertainty of the investigated parameter calculated as:

$$Q_R = \left[\left(\frac{\partial Y}{\partial z_1} Q_1 \right)^2 + \left(\frac{\partial Y}{\partial z_2} Q_2 \right)^2 + \cdots + \left(\frac{\partial Y}{\partial z_n} Q_n \right)^2 \right]^{\frac{1}{2}} \tag{15}$$

The instrumental details are explained in Table 1. The estimated relative uncertainties of the COP, moisture content, drying rate, energy efficiency, SMER, and energy contribution are ±3.39, ±4.23, ±3.60, ±3.58, ±3.28, and ±3.18%, respectively.

Regardless of how precise and accurate a measurement is, it is typically subject to some degree of uncertainty. During the measurement, uncertainty may occur in measurement techniques or in measuring apparatus according to Ahmad and Prakash (2020); assessment of uncertainty is the essential analysis in any experimental work to support the obtained results (Singh *et al.*, 2020a). The total errors were calculated by using Equation 14 according to Gulcimen *et al.* (2016). Table 2 shows the summary of the instruments used and their uncertainty assessment. The total instrument uncertainty W_{th} was found according to the following equation:

$$W_{th} = \sqrt{(Y_1)^2 + (Y_2)^2 + \ldots + (Y_n)^2}$$

(16)

where Y is the independent variable affecting measurements. The total uncertainty for temperature (W_T) measurements from the thermocouple (Z_T) (systematic error from manufacturer) and reading errors (N_T) (random error) follows from Equation 15 according to Gulcimen *et al.* (2016):

$$W_T = \sqrt{(Z_T)^2 + (N_T)^2}$$

(17)

Total uncertainty for measurement of relative humidity (W_{RH}) was determining as follows:

$$W_{RH} = \sqrt{(Z_{RH})^2 + (N_{RH})^2}$$

(18)

Total uncertainties for measurements of solar radiation (W_{SR}), wind (W_{wind}), weighing of products ($W_{weighing}$) and pressure ($W_{pressure}$) of the refrigerant were determined according to AR and Veeramanipriya (2022):

$$W_{SR} = \sqrt{(Z_{SR})^2 + (N_{SR})^2}$$

(19)

$$W_{wind} = \sqrt{(Z_{wind})^2 + (N_{wind})^2}$$

(20)

$$W_{weighing} = \sqrt{(Z_{weighing})^2 + (N_{weighing})^2}$$

(21)

$$W_{pressure} = \sqrt{(Z_{pressure})^2 + (N_{pressure})^2}$$

(22)

The overall total uncertainty in measurement of different parameters according to AR and Veeramanipriya (2022) is given by the following equation:

$$W_{total} = \sqrt{((W_{temp})^2 + (W_{RH})^2 + (W_{SR})^2 + (W_{wind})^2 + (W_{weighing})^2 + (W_{pressure})^2} \quad (23)$$

Table 4:   Equipment and its accuracy, resolution and error

S/N	Equipment	Accuracy	Resolution	Error
1.	Thermocouples	± 0.5 °C	± 0.1 °C	0.14
2.	21CFR Part11 Compliant USB Temperature and Humidity Data Logger Recorder with Free Software.	± 0.3 RH	± 0.1 RH	0.14
3.	Solar Power Meter	± 10 W/m^2	± 0.1 W/m^2	0.14
4.	FST200 Digital RS4850 10 V 0–5 V, Wind Speed Sensor Anemometer Data Logger	± 0.1 m/s	± 0.05 m/s	0.07
5.	Weight balance	± 0.14 g	± 0.1 g	0.14
6.	Pressure gauge	± 0.1 psi	± 0.1 psi	0.14

CHAPTER FOUR

RESULTS AND DISCUSSION

4.1   Uncertainty Analysis

The total uncertainties in the measuring instruments and reading errors was calculated according to Equation 23 and found to be ± 1.5% (rounded); this value is small as compared to the acceptable range of ±10% according to Choi *et al.* (2018).

4.1.1   Drying Temperature and Moisture Content

Drying air temperature measured with the thermocouple in the drying chamber versus time for three configurations is shown in Fig. 10. The starting point (0 min) corresponded to 0900 h and the experiment was finished at 1000 h (600 min on the plots). In general, for the fully open system, the drying air temperature was higher due to the contribution of surroundings, whereas in partially and fully closed systems the temperature was lower because of cool air contribution from the evaporator circulating through the system. A decrease in drying temperature was observed in the first 100 minutes which was possible due to the evaporation of rather a big amount of water from wet tobacco leaves; air temperature decreased rapidly during the initial drying period for the fully open system. The drying air temperature depends on heated air from the heat pump condenser and the heated air is delivered into the solar collector. The mass of evaporated water from 15 kg of tobacco leaf load with time is shown in Fig. 11; it can be observed that for all three systems, the dry product was obtained after the same drying time, about 400 min, and approximately 12 kg of water was evaporated.
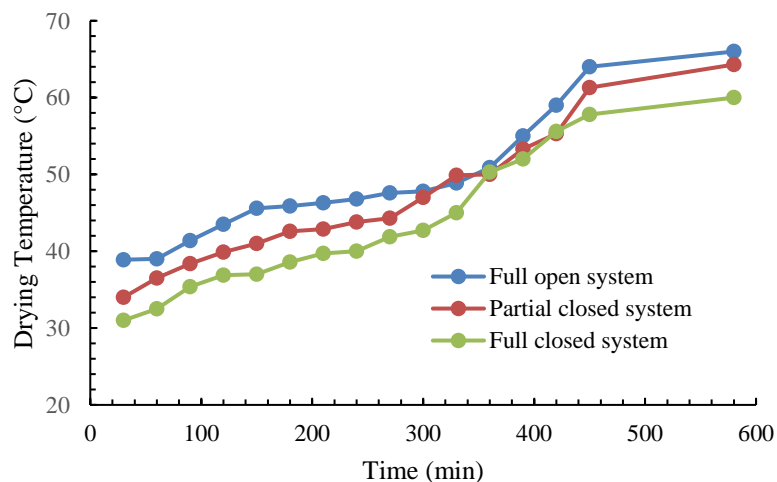

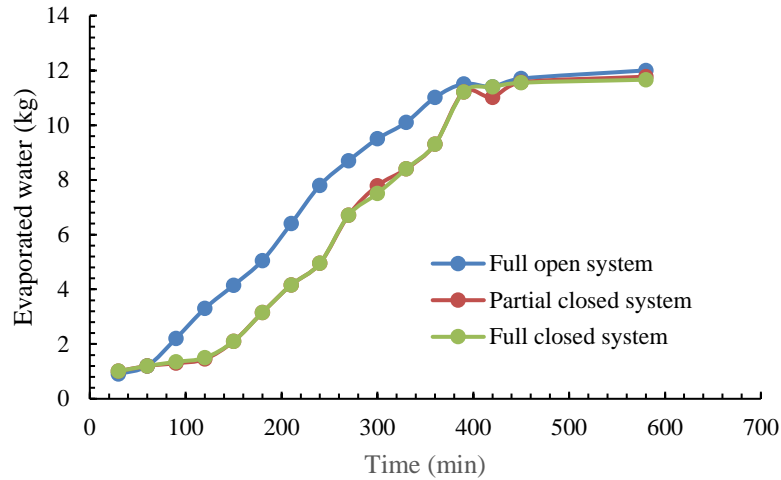**Figure 9:   Drying air temperature with time**

Figure 10: Mass of evaporated water vs. drying time

Solar irradiance and ambient temperature being dependent on the climatic condition are very important parameters for drying tobacco leaves in the SAHPD. The solar irradiance was measured during a day when the fully open system experiment was conducted as shown in Fig. 12, similar trends were observed for both parameters, and the maximum values of 670 W/m² and 32°C were detected for solar irradiance and ambient temperatures, respectively, close to midday.
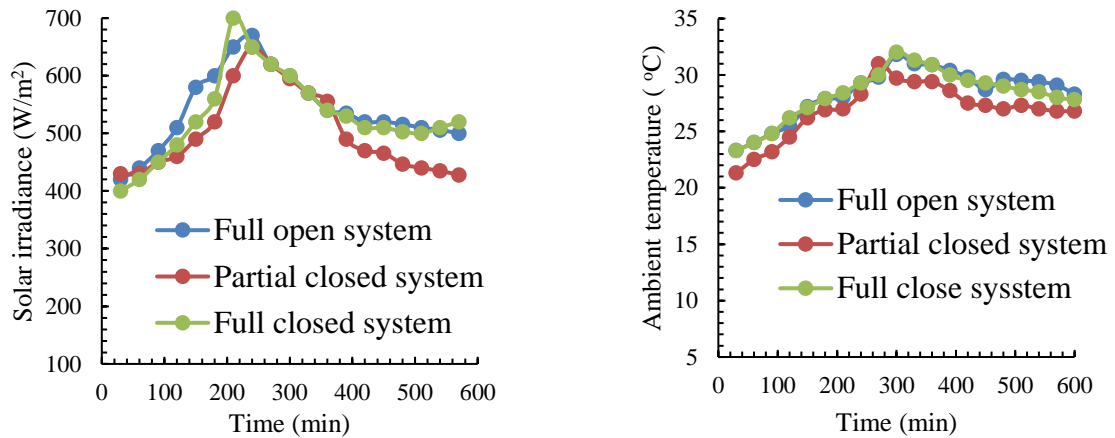

Figure 11: The variation of solar irradiation (a) and ambient temperature (b) with time

4.2 Performance of the SAHP

4.2.1 Solar thermal efficiency

The solar thermal efficiency calculated using Equation 1 differs throughout the day depending on the air duct configuration; the highest efficiency was recorded for the fully open-air duct system (69.3%) followed by a partially and completely closed system which were 66.3 and 64.8%, respectively. The minimum thermal efficiency was 22.5, 21.5, and 20.8%, respectively. The thermal efficiency of solar collector varies when solar irradiance varies. The solar collector was more sensitive to solar irradiance; the solar thermal efficiency was higher for higher solar irradiance. The lower thermal efficiency recorded for the fully closed system possibly was due to the circulation of cold air from the evaporator while the fully open system was favored by high ambient temperature.

The relative humidity in the drying chamber vs. drying time is depicted in Fig. 13; maximum values were 45.5, 43.9, and 43.7% for the fully open, partially closed, and fully closed systems, respectively, while minimum humidity values were equal to 28.7, 30.7, and 33.1%. Whenever the drying temperature increased the relative humidity also decreased (Ju *et al.,* 2018).
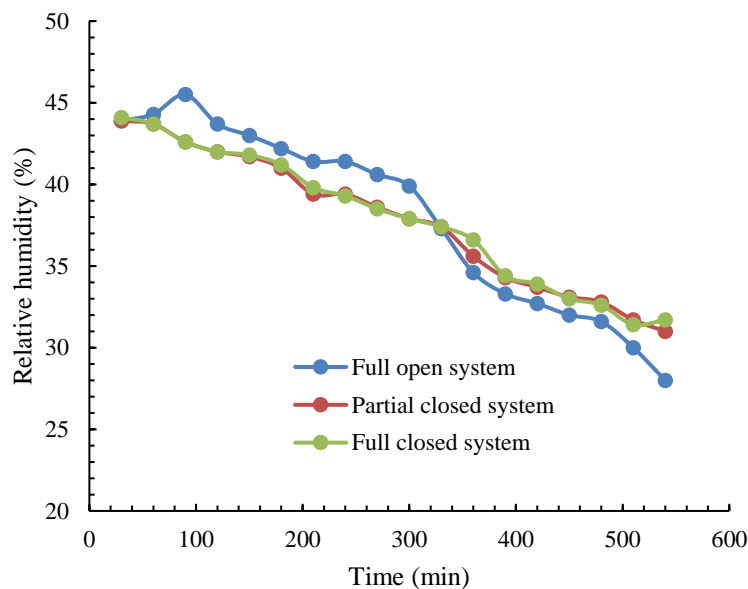

Figure 12:   The relative humidity in the drying chamber vs. drying time

For the partially and fully closed systems, as compared to the fully open system, the evaporator fans significantly affected both the relative humidity and drying temperature in the drying chamber because of the circulation of cold air from the evaporator (Krishnamoorthy *et al.,*

2017). The thermal efficiency of the dryer versus drying time is shown in Fig. 14. The drying efficiency was higher for moist tobacco leaves and was decreasing as the moisture reduced. The higher drying efficiency is produced when the humidity decreases due to increase of the drying temperature (Singh *et al.,* 2020b). Maximum drying efficiency of about 65% was observed for the fully open system.
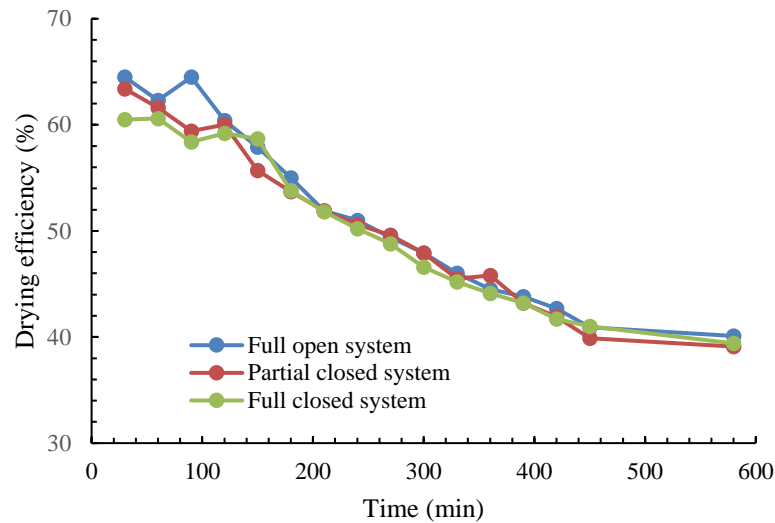

Figure 13:   The thermal efficiency of a dryer vs. time

The drying rate of the dryer for the three configurations is demonstrated in Fig. 14; the average values are 1.5, 1.4, and 1.3 kg/h for fully open, partially-open, and fully closed systems, respectively. The drying rate of the fully closed system starts to increase with time due to the increase of the drying temperature to a maximum and then decreases when moisture is reduced in the tobacco leaves. Initially**,** for some time**,** the drying rate of the fully open system started to decrease due to the low inlet temperature, and then increases with time up when the inlet temperature and dryer temperature were higher than the drying rate due to reduced moisture. It is worth noting that the highest drying rate was observed for the fully open system**;** this is because it exhibited higher drying temperatures and low relative humility.
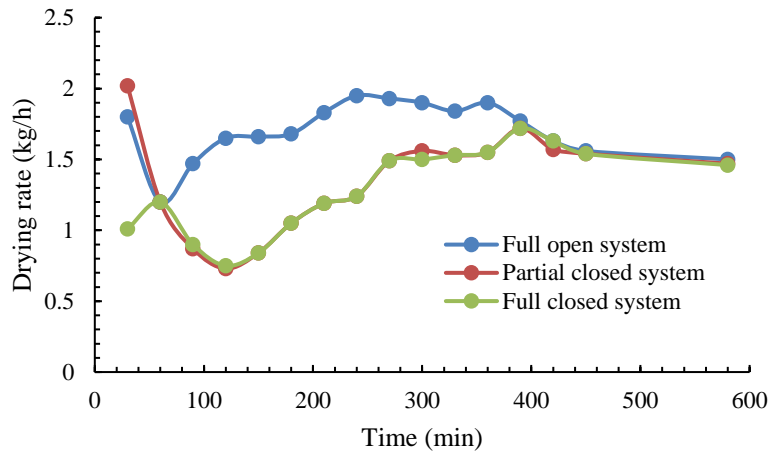
Figure 14: Drying rate vs. time

4.2.2 Performance of Vapor Compression Heat Pump

The coefficient of performance of the heat pump as calculated by Equation 2 for the open, partially closed, and fully closed air duct systems is shown in Fig. 16. The average values of the COP_{hp} were 3.4, 3.2, and 3.0 for the open, partially closed, and fully closed air duct systems, respectively. The condenser's inlet and outlet temperatures were influenced by the surrounding conditions; the average inlet and outlet temperatures were between 28.2 and 48.4°C; 27.4 and 46.5°C; 24.4 and 43.5°C for the fully open, partially closed, and fully closed system, respectively. The mixing of ambient air and cold air from the evaporator affects the condenser outlet temperature range to low values in partially and fully closed ducted system configurations, but open systems use only ambient air as the condenser inlet. The circulated air from the evaporator causes the COP_{hp} to fluctuate and affect the dryer heating capacity.

The $COP_{overall}$ of the three configurations is shown in Fig. 17; the minimum and maximum $COP_{overall}$ for the fully opened, partially closed, and completely closed system was 2.6 to 3.2, 2.1 to 2.5, and 2.3 to 2.9, respectively, which were calculated using Equation 3. The $COP_{overall}$ increased with the solar irradiance increase and reduced when solar irradiance was low (Luo *et al.,* 2020). The $COP_{overall}$ for the open-air duct system was higher than for the other two systems. The $COP_{overall}$ was lower as compared to COP_{hp} because of the inclusion of energy consumed by the evaporator and condenser fans in the calculation. Thus, the greater values of the COP_{hp} and $COP_{overall}$ were observed for the fully open system.
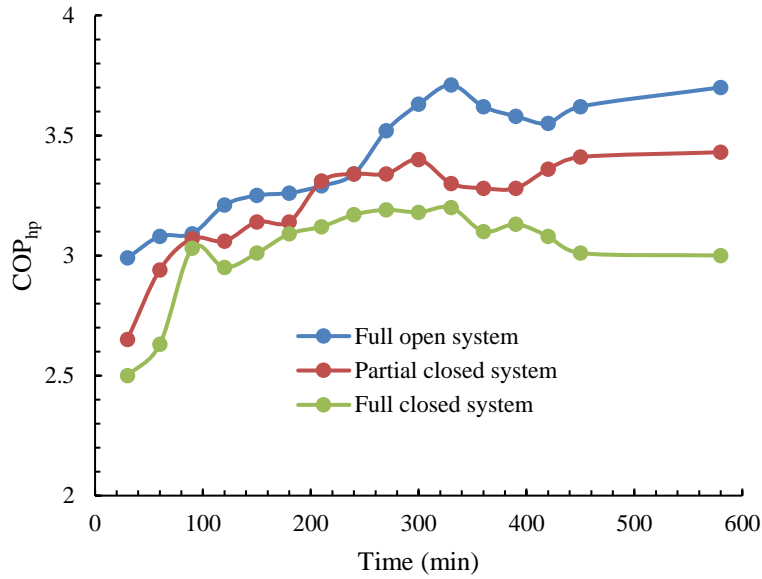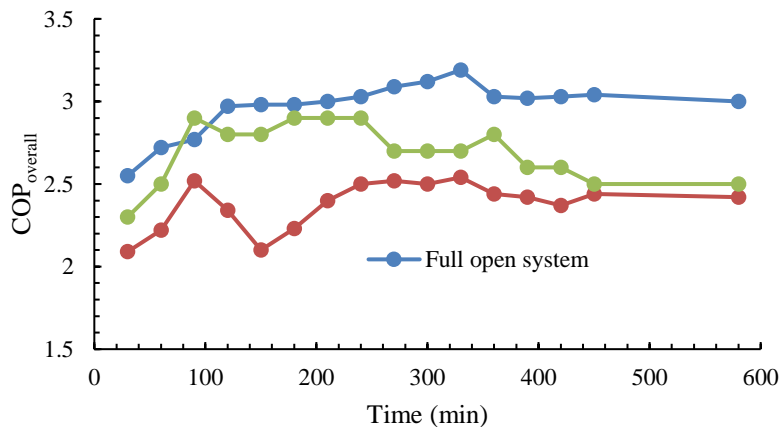
Figure 15: Variation of COPhp with drying time

Figure 16: Variation of the overall coefficient of performance of the SAHPD with drying time

4.2.3   Heat Energy Contribution

Heat energy contributions made by the solar collector and condenser as calculated using Equations 9 and 10 are shown in Figs. 18 and 19. The average values for the solar collector were 6.6, 5.0, and 5.1%, while for the condenser were 93.4, 95.0, and 94.9%, for the open, partially closed, and fully closed systems, respectively. Solar radiation and the temperature difference between the solar collector's inlet and outlet had an impact on the heat energy contribution. The percentage of the heat energy contribution made by the condenser is increased with a decrease in the contribution of the solar collector which is in accordance with the literature (Li *et al.,* 2019).
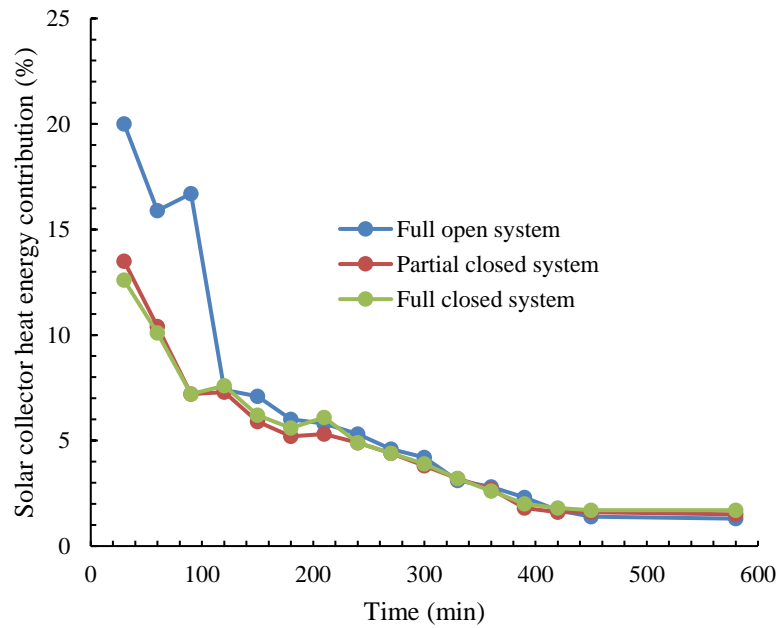
Figure 17:   Variation of solar collector heat energy contribution with time
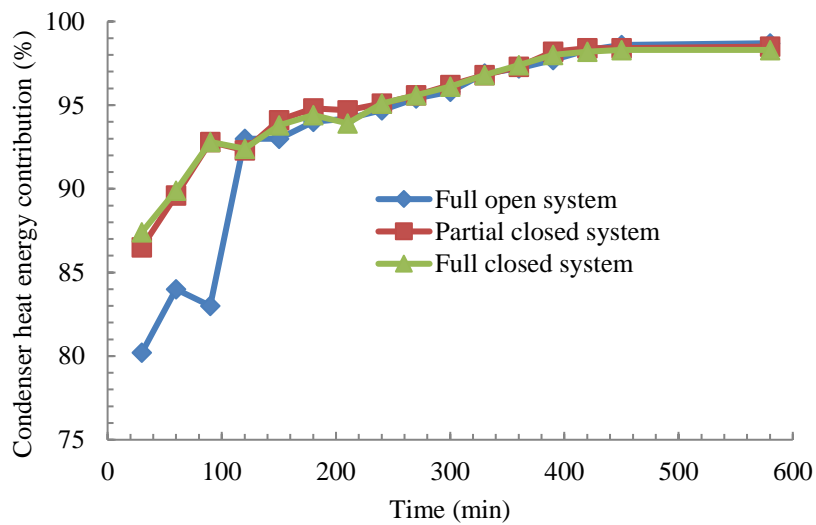
Figure 18:   Variation of the heat energy contribution of the condenser with time

The SAHPD has been made and used for drying of various biomaterials in different countries with different climatic conditions and it was observed that COP_{hp} varied from 2.28 to 4.18 as reported by Koşan *et al.* (2020). The SAHPD was conducted for three distinct weather conditions such as clear day, intermittent cloudy day, and overcast sky.

CHAPTER FIVE

CONCLUSON AND RECOMMMENDATIONS

5.1   Conclusion

The present study investigated the influence of duct configurations on the performance of the developed Solar-Assisted Heat Pump Dryer (SAHPD) for drying tobacco leaves (commercial crop). Three air duct configurations (fully open, partially closed, and fully closed) were investigated and the best confirmation was identified. In comparison to partially and fully closed systems, the fully open system was found to have a greater drying rate, 1.5 kg/h, and higher COP_{hp}, ranging from 3.0 to 3.7 while the drying rate was 1.4, and 1.3 kg/h, and the COP was 3.2 and 3.0, respectively for partial closed and fully closed system. Partially and fully closed systems demonstrated lower drying performance than fully open system because of the circulation of cold air and higher relative humidity of the drying air. While the evaporator fan impacts the temperature of air circulating in the duct in partially and totally closed systems, it increases energy consumption owing to heat recovery. The fully open systems require less resources. Therefore, for drying tobacco leaves, the fully open design outperformed the partially and completely closed configurations.

5.2   Recommendations

The fully open system performs well but for Future studies should focus on comprehensive investigation of the life cycle and technoeconomic of solar-assisted heat pump dryers integrated with duct, which may provide a global view of the environmental and economic effects.

REFERENCES

Ahmad, A., & Prakash, O. (2020). Performance evaluation of a solar greenhouse dryer at different bed conditions under passive mode. *Journal of Solar Energy Engineering*, *142*(1), 011006.

Alishah, A., Kiamahalleh, M. V., Yousefi, F., Emami, A., & Kiamahalleh, M. V. (2018). Solar-Assisted Heat Pump Drying of Coriander: An Experimental Investigation. *International Journal of Air-Conditioning and Refrigeration,* 26**,** 1850037.

AR, U. S., & Veeramanipriya, E. (2022). Performance evaluation, morphological properties and drying kinetics of untreated Carica Papaya using solar hybrid dryer integrated with heat storage material. *Journal of Energy Storage*, *55*, 105679.

Boateng, I. D. (2023). A review of solar and solar-assisted drying of fresh produce: State of the art, drying kinetics, and product qualities. *Journal of the Science of Food and Agriculture*.

Chacha, B. K. (2000). From Pastoralists to Tobacco Peasants: The British American Tobacco (BAT) and Socio-ecological Change in Kuria District, Kenya, 1969-1999. *Njoro: Egerton University*.

Chegini, G., Khayaei, J., Rostami, H., & Sanjari, A. (2007). Designing of a heat pump dryer for drying of plum. *Journal of Research and Applications in Agricultural Engineering,* 52**,** 63-65.

Choi, Y., Choi, M., Kim, M., Ha, J. W., Kim, S., & Choo, J. (2018). Stargan: Unified generative adversarial networks for multi-domain image-to-image translation. *Proceedings of the IEEE Conference on Computer Vision and Pattern Recognition*, 8789-8797.

Chou, S., & Chua, K. (2001). New hybrid drying technologies for heat sensitive foodstuffs. *Trends in Food Science & Technology,* 12**,** 359-369.

Chou, S., Chua, K., Hawlader, M., & Ho, J. (1998). A Two-Stage Heat Pump Dryer for Better Heat Recovery and Product Quality. *Journal of The Institute of Engineers, Singapore,* 38**,** 8-14.

Chua, K., Mujumdar, A., Chou, S., Hawlader, M., & Ho, J. (2000). Convective Drying of Banana, Guava and Potato Pieces: Effect of Cyclical Variations of Air Temperature on Drying Kinetics and Color Change. *Drying Technology,* 18**,** 907-936.

Chua, K. J., & Chou, S. K. (2014). Recent advances in hybrid drying technologies. *Emerging Technologies for Food Processing*, 447-459.

DeSolaPool, I. (2009). *Technologies of Freedom*, Harvard University Press.

Fara, V., Grigorescu, R., Marinescu, P., & Dogărescu, V. (1985). Experimental Results at a Pilot Solar Station Used for Curing Tobacco in a Bulk-Curing System—Economic Implications. *Energy in Agriculture,* 4, 41-55.

Gulcimen, F., Karakaya, H., & Durmus, A. (2016). Drying of sweet basil with solar air collectors. *Renewable Energy*, *93*, 77-86.

Hawlader, M., Chou, S., Jahangeer, K., Rahman, S., & Kw, E. L. (2003). Solar-Assisted Heat-Pump Dryer and Water Heater. *Applied Energy,* 74, 185-193.

Hawlader, M., & Jahangeer, K. (2006). Solar heat pump drying and water heating in the tropics. *Solar Energy,* 80, 492-499.

Hawlader, M., Perera, C. O., & Tian, M. (2006). Properties of modified atmosphere heat pump dried Foods. *Journal of Food Engineering,* 74, 392-401.

Huy, B. Q. (2018). Experiment investigation on a solar asisted heat pump dryer for Chili. *International Journal of Energy and Environmental Science,* 3, 37.

Ingvald, S., Mmen, I., & Kramer, K. (1994). New applications of heat pumps in drying processes. *Drying Technology,* 12, 889-901.

Jangam, S. V., & Thorat, B. N. (2010). Optimization of Spray Drying of Ginger Extract. *Drying Technology,* 28, 1426-1434.

Jimu, L., Mataruse, L., Musemwa, L., & Nyakudya, I. W. (2017). The Miombo Ecoregion up in Smoke: The Effect of Tobacco Curing. *World Development Perspectives,* 5**,** 44-46.

Ju, H. Y., Zhao, S. H., Mujumdar, A., Fang, X. M., Gao, Z. J., Zheng, Z. A., & Xiao, H. W. (2018). Energy efficient improvements in hot air drying by controlling relative

humidity based on weibull and bi-di models. *Food and Bioproducts Processing,* 111**,** 20-29.

Kaewkiew, J., Nabnean, S., & Janjai, S. (2012). Experimental investigation of the performance of a large-scale greenhouse type solar dryer for drying chilli in Thailand. *Procedia Engineering*, *32*, 433-439.

Kägi, W., & Schmid, M. (2010). *Tobacco and forests–the role of the tobacco industry regarding deforestation, afforestation and reforestation*. Technical report, Basel: BSS Economic Consultants.

Kivevele, T., & Huan, Z. (2014). A review on opportunities for the development of heat pump drying systems in South Africa. *South African Journal of Science*, *110*(5-6), 01-11.

Kivevele, T., & Huan, Z. (2014). A review on opportunities for the development of heat pump drying systems in South Africa. *South African Journal of Science*, *110*(5-6), 01-11.

Koşan, M., Demirtaş, M., Aktaş, M., & Dişli, E. (2020). Performance analyses of sustainable PV/T assisted heat pump drying system. *Solar Energy*, *199*, 657-672.

Krishnamoorthy, S., Modera, M., & Harrington, C. (2017). Efficiency optimization of a variable-capacity/variable-blower-speed residential heat-pump system with ductwork. *Energy and Buildings*, *150*, 294-306.

Kush, E. A. (1980). *Performance of heat pumps at elevated evaporating temperatures: With application to solar input*. Brookhaven National Lab., Upton, New York (USA).

Li, C., Liu, J., Zheng, S., Chen, X., Li, J., & Zeng, Z. (2019). Performance analysis of an improved power generation system utilizing the cold energy of LNG and solar energy. *Applied Thermal Engineering*, *159*, 113937.

Lingayat, A. B., Chandramohan, V. P., Raju, V. R. K., & Meda, V. (2020). A review on indirect type solar dryers for agricultural crops: Dryer setup, its performance, energy storage and important highlights. *Applied Energy*, *258*, 114005.

Liu, X., Ni, L., Lau, S. K., & Li, H. (2013). Performance analysis of a multi-functional heat pump system in heating mode. *Applied Thermal Engineering*, *51*(1-2), 698-710.

Luo, B., Zou, P., Jiang, T., Gao, Q., & Liu, J. (2020). Decoupled duplex Stirling machine: Conceptual design and theoretical analysis. *Energy Conversion and Management*, *210*, 112704.

Luo, B., Zou, P., Jiang, T., Gao, Q., & Liu, J. (2020). Decoupled Duplex Stirling Machine: Conceptual Design And Theoretical Analysis. *Energy Conversion And Management,* 210**,** 112704.

Msigwa, F. J. (2019). *Impacts of tobacco production on forest resources management in Kasulu District, Tanzania* (Doctoral dissertation, The Open University of Tanzania).

Mujumdar, A. S. (2006). *Handbook Of Industrial Drying*, Crc Press.

Munanga, W., Mugabe, F., Kufazvinei, C., & Svotwa, E. (2014). Evaluation of the curing efficiency of the rocket barn in Zimbabwe. *International Journal of Agriculture Innovations and Research*, *3*(2), 2319-1473.

Naemsai, T., Jareanjit, J., & Thongkaew, K. (2019). Experimental investigation of solar-assisted heat pump dryer with heat recovery for the drying of chili peppers. *Journal of Food Process Engineering*, *42*(6), e13193.

Newbert, G. J. (1985). Energy efficient drying, evaporation and similar processes. *Journal of Heat Recovery Systems, 5*(6), 551-559.

O'Neill, M. B., Rahman, M. S., Perera, C. O., Smith, B., & Melton, L. D. (1998). Color and density of apple cubes dried in air and modified atmosphere. *International Journal of Food Properties*, *1*(3), 197-205.

Phoungchandang, S. (2009). Simulation model for heat pump-assisted dehumidified air drying for some herbs. *World Journal of Agriculture Sciences*, *5*(2), 138-142.

Ratner, S., Gomonov, K., Revinova, S., & Lazanyuk, I. (2020). Energy saving potential of industrial solar collectors in Southern Regions of Russia: The case of Krasnodar Region. *Energies*, *13*(4), 885.

Sagar, V. R., & Kumar, P. S. (2010). Recent advances in drying and dehydration of fruits and vegetables: A review. *Journal of Food Science and Technology*, *47*, 15-26.

Şevik, S. (2014). Experimental investigation of a new design solar-heat pump dryer under the different climatic conditions and drying behavior of selected products. *Solar Energy*, *105*, 190-205.

Şevik, S. (2014). Experimental investigation of a new design solar-heat pump dryer under the different climatic conditions and drying behavior of selected products. *Solar Energy*, *105*, 190-205.

Shanmugam, V., & Natarajan, E. (2007). Experimental study of regenerative desiccant integrated solar dryer with and without reflective mirror. *Applied thermal Engineering*, *27*(8-9), 1543-1551.

Singh, A., Sarkar, J., & Sahoo, R. R. (2020). Experimental energy, exergy, economic and exergoeconomic analyses of batch-type solar-assisted heat pump dryer. *Renewable Energy*, *156*, 1107-1116.

Singh, A., Sarkar, J., & Sahoo, R. R. (2020b). Experimental performance analysis of novel indirect-expansion solar-infrared assisted heat pump dryer for agricultural products. *Solar Energy*, *206*, 907-917.

Singh, A., Sarkar, J., & Sahoo, R. R. (2020c). Experimentation on solar-assisted heat pump dryer: Thermodynamic, economic and exergoeconomic assessments. *Solar Energy*, *208*, 150-159.

Srisittipokakun, N., Kirdsiri, K., & Kaewkhao, J. (2012). Solar drying of Andrographis paniculata using a parabolicshaped solar tunnel dryer. *Procedia Engineering*, *32*, 839-846.

Theerakulpisut, S. (1990). *Modelling Heat Pump Grain Drying Systems.*

Tjukup Marnoto, M., Endang Sulistyowati, S., Mahreni, M., & Syahri, M. (2012). The Characteristic of Heat Pump Dehumidifier Drier in the Drying of Red Chili (*Capsium annum L.*). *International Journal of Science and Engineering, 3*(1), 22-25.

Vickers, N. J. (2017). Animal communication: When I'm calling you, will you answer too?. *Current Biology*, *27*(14), R713-R715.

Xu, B., Wang, D., Li, Z., & Chen, Z. (2021). Drying and dynamic performance of well-adapted solar assisted heat pump drying system. *Renewable Energy*, *164*, 1290-1305.
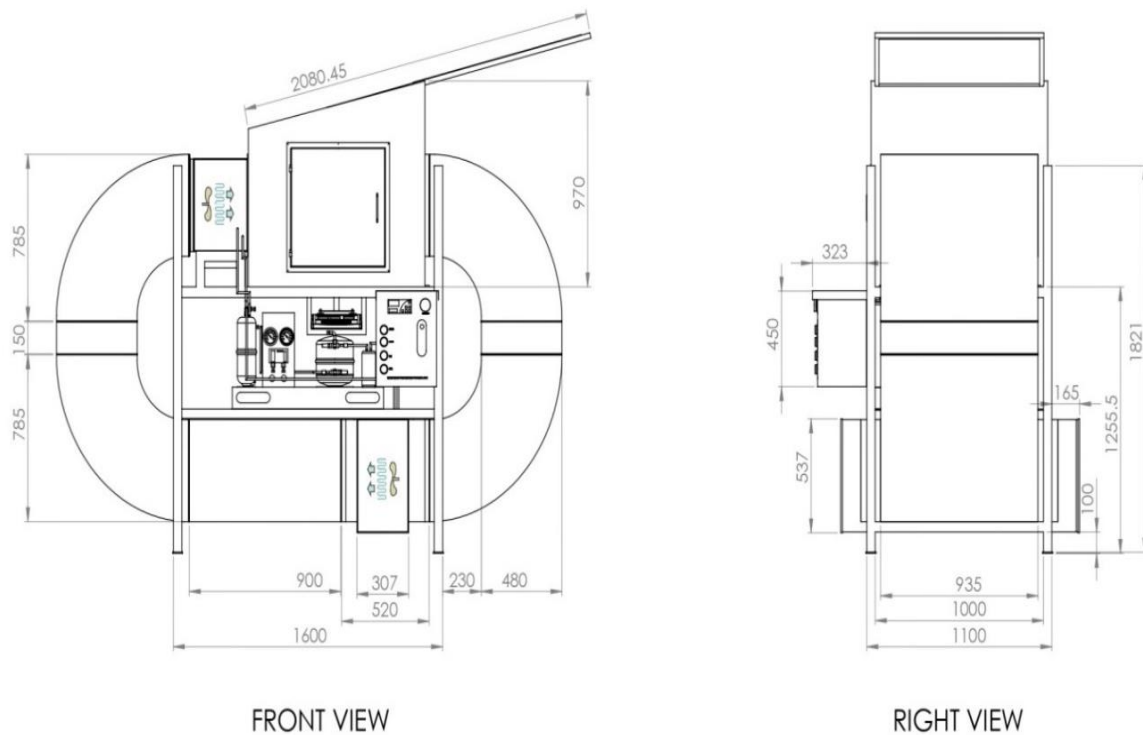
Yahya, M., Fahmi, H., Hasibuan, R., & Fudholi, A. (2023). Development of hybrid solar-assisted heat pump dryer for drying paddy. *Case Studies in Thermal Engineering*, *45*, 102936.
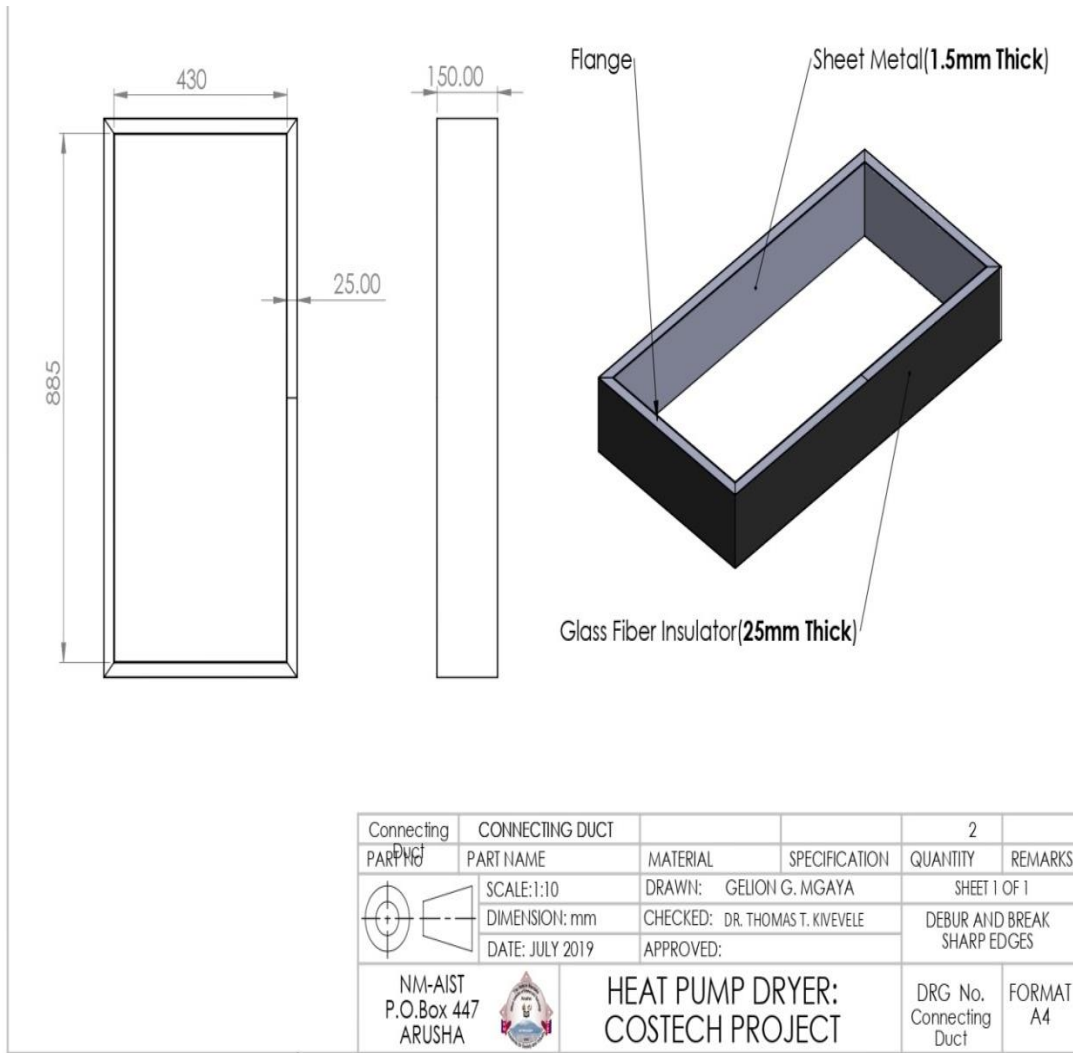
APPENDICES

Appendix 1: Detail Drawings of Solar Assistance Heat Pump Dryer

The solar assistance heat pump dryer contains several components which were designed and drawn. The detailed drawings of each component are shown below. All these parts form the complete SAHPD.
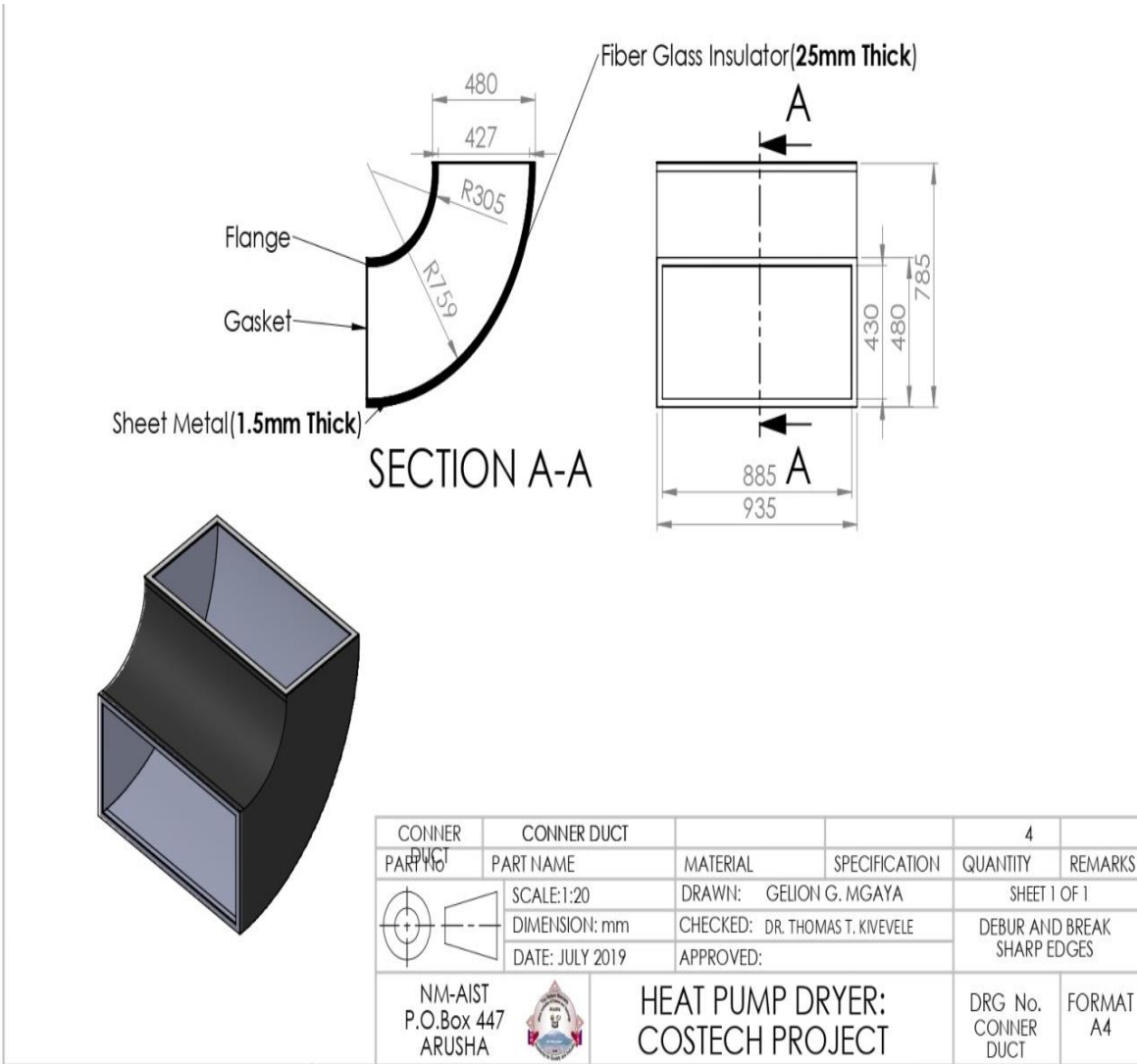
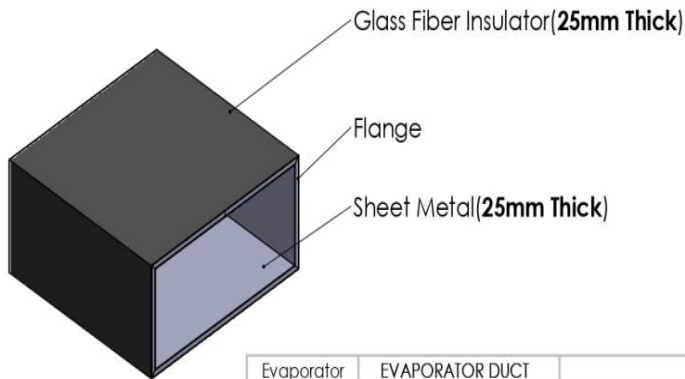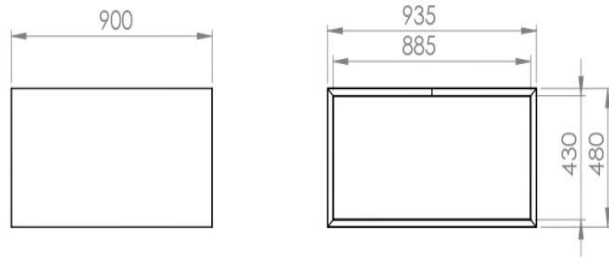## (i) Front and right view of main drawing dimension

FRONT VIEW   RIGHT VIEW

(ii)   Labelled connecting duct

Connecting Duct	CONNECTING DUCT				2	
PART NO	PART NAME	MATERIAL	SPECIFICATION	QUANTITY		REMARKS
	SCALE:1:10	DRAWN: GELION G. MGAYA		SHEET 1 OF 1		
	DIMENSION: mm	CHECKED: DR. THOMAS T. KIVEVELE		DEBUR AND BREAK SHARP EDGES		
	DATE: JULY 2019	APPROVED:				
NM-AIST P.O.Box 447 ARUSHA		HEAT PUMP DRYER: COSTECH PROJECT		DRG No. Connecting Duct	FORMAT A4	

(iii)   Labelled corner duct

Fiber Glass Insulator(**25mm Thick**)

480
427
R305
R759
Flange
Gasket
Sheet Metal(**1.5mm Thick**)

SECTION A-A

A
785
430
480
885 A
935

CONNER DUCT PART No	CONNER DUCT			4	
	PART NAME	MATERIAL	SPECIFICATION	QUANTITY	REMARKS
	SCALE:1:20	DRAWN: GELION G. MGAYA		SHEET 1 OF 1	
	DIMENSION: mm	CHECKED: DR. THOMAS T. KIVEVELE		DEBUR AND BREAK SHARP EDGES	
	DATE: JULY 2019	APPROVED:			
NM-AIST P.O.Box 447 ARUSHA		HEAT PUMP DRYER: COSTECH PROJECT		DRG No. CONNER DUCT	FORMAT A4

39

(iv) Labelled evaporator duct

Evaporator Duct	EVAPORATOR DUCT					
PART No	PART NAME		MATERIAL	SPECIFICATION	QUANTITY	REMARKS
		SCALE:1:20	DRAWN: GELION G. MGAYA		SHEET 1 OF 1	
		DIMENSION: mm	CHECKED: DR. THOMAS T. KIVEVELE		DEBUR AND BREAK SHARP EDGES	
		DATE: JULY 2019	APPROVED:			
NM-AIST P.O.Box 447 ARUSHA			HEAT PUMP DRYER: COSTECH PROJECT		DRG No. Evaporator Duct	FORMAT A4

Labels on isometric view:
- Glass Fiber Insulator(**25mm Thick**)
- Flange
- Sheet Metal(**25mm Thick**)

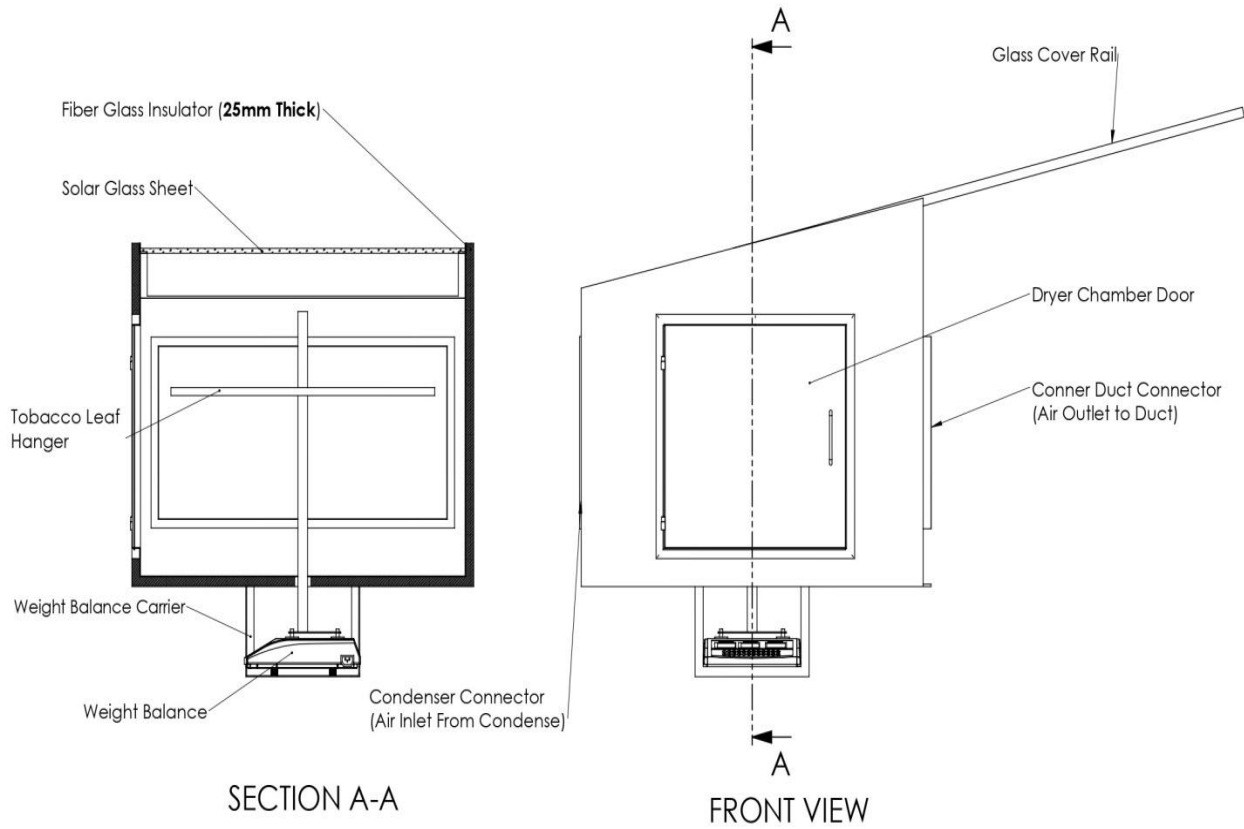Dimensions: 900, 935, 885, 430, 480

(v)   Isometric view of SAHPD
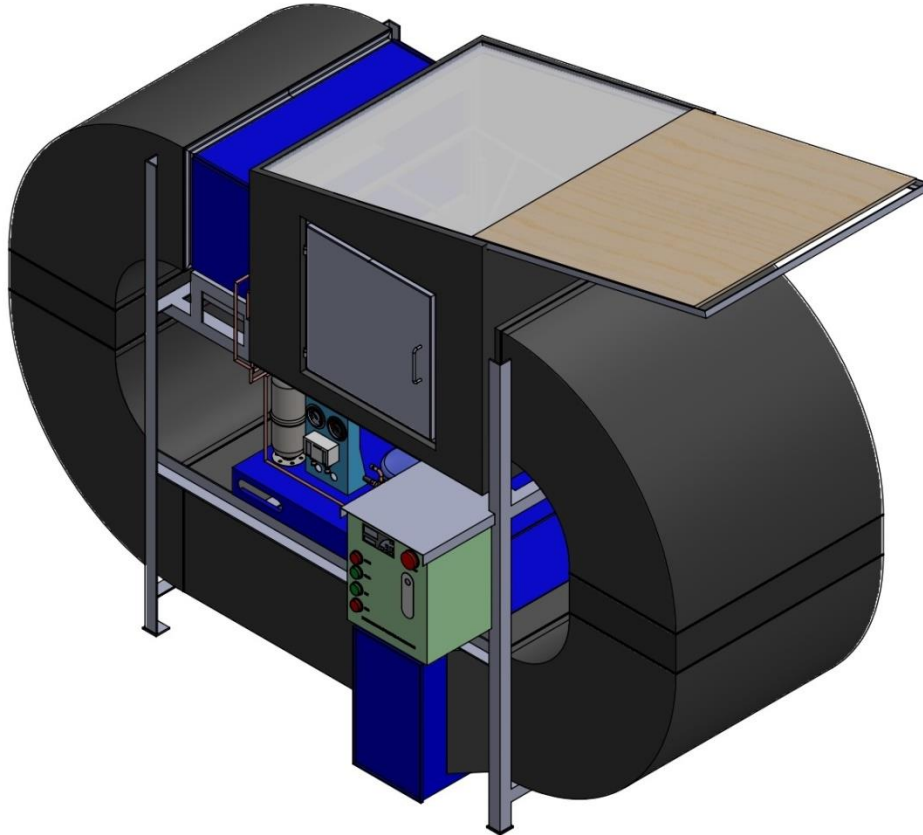
ISOMETRIC VIEW

(vi)   Isometric view of drying chamber
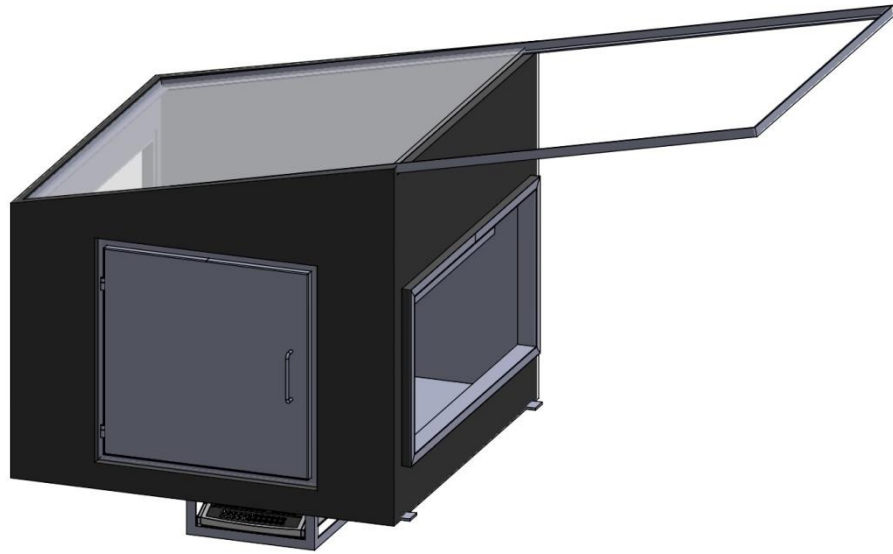
ISOMETRIC VIEW

(vii)   Front view section drawing of drying chamber

Fiber Glass Insulator (**25mm Thick**)

Solar Glass Sheet

Tobacco Leaf Hanger

Weight Balance Carrier

Weight Balance

Condenser Connector (Air Inlet From Condense)

SECTION A-A

A

Glass Cover Rail

Dryer Chamber Door

Conner Duct Connector (Air Outlet to Duct)

A

FRONT VIEW

(viii)   Right view section drawing of drying chamber

SECTION N-N

RIGHT VIEW
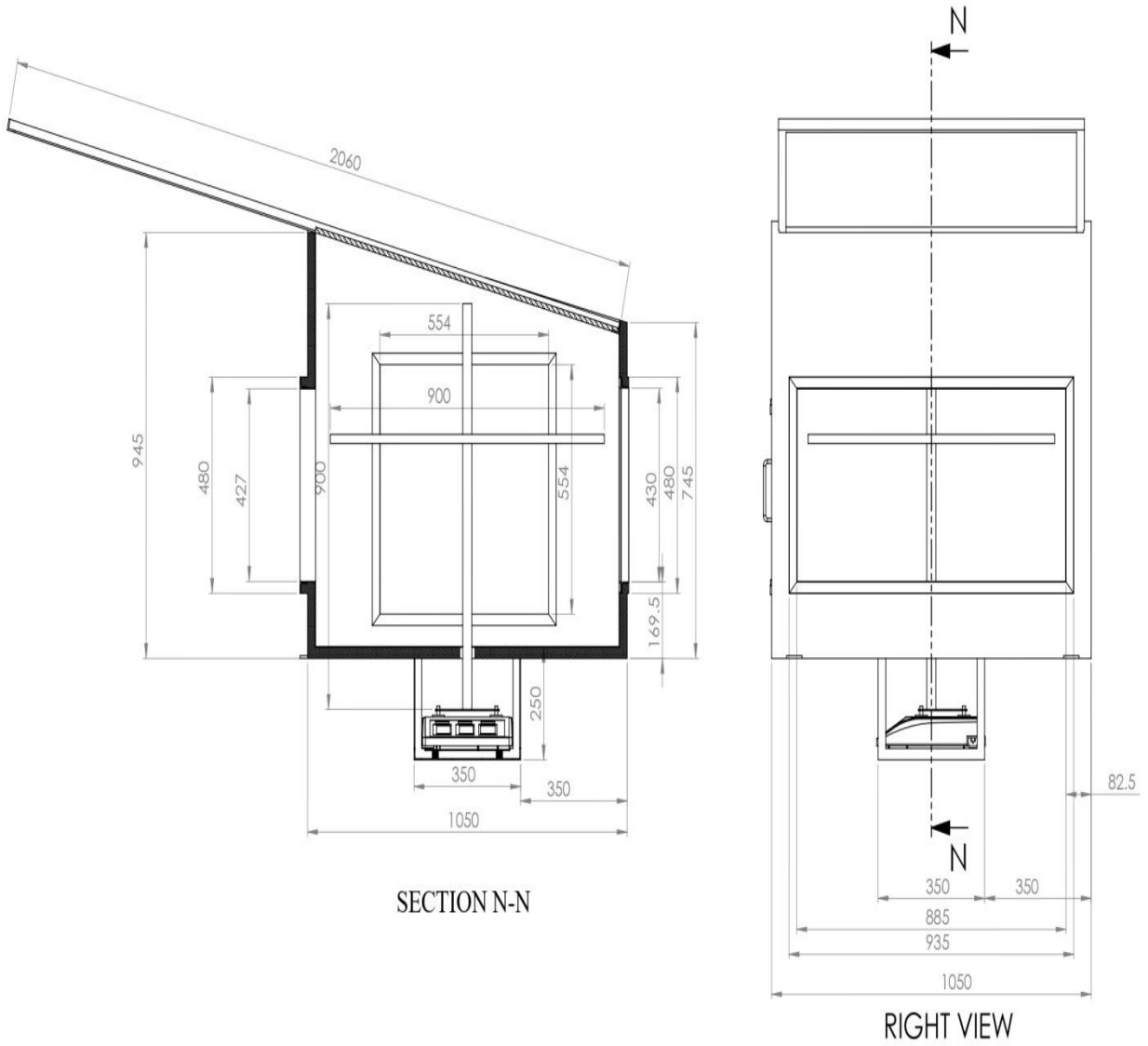
(ix)   Partially closed picture of SAHPD

RESEARCH OUTPUTS

(i)   **Journal Paper**

Suleiman, S. A., Pogrebnoi, A., & Kivevele, T. T. (2023). Influence of Duct Configurations on the Performance of Solar-Assisted Heat Pump Dryer for Drying Tobacco Leaves. *International Journal of Photoenergy*, *2023*.

(ii)   **Poster Presentation**

Appendix 2:   Poster Presentation

Influence of duct configurations on the performance of solar-assisted heat pump dryer for drying tobacco leaves

Salum A. Suleiman[1], Alexander Pogrebnoi[2], Thomas T. Kivevele[3]

Introduction

Drying is the key process to maintain quality without deteriorating biomaterial product and maintain original taste and uphold the nutrition values. Many researchers suggest the use of heat pump dryers because of their high efficiency and energy-saving potential and less negative impact on the environment and they preserve the quality of the dried product. To increase the performance of heat pump dryer, solar collectors are integrated into the heat pump system to form a solar-assisted heat pump dryer (SAHPD). The SAHPD application provides high energy efficiency with controllable temperature, airflow, air humidity, and enormous energy-saving potential. However, SAHPDs are affected by the change in ambient conditions, proper configuration of the duct is therefore a key in improving the performance of the dryer. Therefore, the present study.

Conclusion

The present study investigated the influence of duct configurations on the performance of the developed Solar-Assisted Heat Pump Dryer (SAHPD) for drying tobacco leaves. Three air duct configurations (fully open, partially closed, and fully closed) were investigated. In comparison to partially and fully closed systems, the fully open system was investigates the influence of duct configurations on the thermal performance of the SAHPD for drying agricultural products. In this study the developed SAHPD is tested for drying tobacco leaves.

Problem statement

The tobacco sector in Tanzania is being accused of destroying forests by cutting trees to obtain wood for curing tobacco leaves, causing a threat of deforestation and global warming in the country.

Methodology
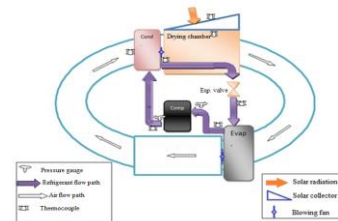
Schematic diagram of Full open system

found to have a greater drying rate, 1.5 kg/h, and higher COP_{hp}, ranging from 3.0 to 3.7 while the drying rate was 1.4, and 1.3 kg/h, and the COP was 3.2 and 3.0, respectively for partial closed and fully closed system. Therefore, for drying tobacco leaves, the fully open design outperformance of the partially and completely closed configurations.